Inorganic Chemistry
Article
Cite This: Inorg. Chem. 2019, 58, 8357−8368
pubs.acs.org/IC

Selective Activation of CH Bonds in Polar Vinyl Olefins and Coupling of Ethylene to the Activated Carbon Atoms in Pentaruthenium Complexes

Richard D. Adams,* Mark D. Smith, Jonathan D. Tedder, and Nutan D. Wakdikar

Department of Chemistry and Biochemistry, University of South Carolina, Columbia, South Carolina 29208, United States

S *Supporting Information*

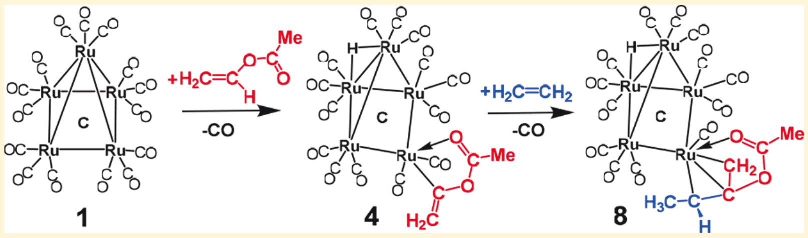

ABSTRACT: $Ru_5(\mu_5\text{-}C)(CO)_{15}$, **1**, has been found to activate CH bonds in the vinyl group of polar vinyl olefins, methyl acrylate (MA), and vinyl acetate (VAc), through a cluster opening process to yield the complexes $Ru_5(\mu_5\text{-}C)(CO)_{14}[\eta^2\text{-}O{=}C(OMe)CH{=}CH](\mu\text{-}H)$, **2**, and $Ru_5(\mu_5\text{-}C)(CO)_{14}[\eta^2\text{-}(MeCO_2)C{=}CH_2](\mu\text{-}H)$, **4**, respectively. The site of CH activation is dependent on the olefin substituent. In **2**, the site of CH activation is the β-carbon atom of the vinyl group, while in **4** the CH activation has occurred exclusively at the α-carbon atom of the vinyl group. Compound **2** can be further decarbonylated to yield the complex $Ru_5(\mu_5\text{-}C)(CO)_{13}[\mu\text{-}\eta^3\text{-}O{=}C(OMe)CHCH](\mu\text{-}H)$, **3**, which contains a η^3-bridging acryloyl ligand. Compound **2** reacts with ethylene in the presence of Me_3NO to yield three new Ru_5 products: $Ru_5(\mu_5\text{-}C)(CO)_{13}[\eta^4\text{-}1\text{-}\textit{anti},3\text{-}\textit{syn}\text{-}\{O{=}C(OMe)\}C(H)C(H)C(H)Me](\mu\text{-}H)$, **5**, $Ru_5(\mu_5\text{-}C)(CO)_{12}(C_2H_4)[\mu\text{-}\eta^3\text{-}O{=}C(OMe)C(H)C(H)](\mu\text{-}H)$, **6**, and $Ru_5(\mu_5\text{-}C)(CO)_{13}[\eta^4\text{-}\textit{anti}\text{-}O{=}C(OMe)H_2CHCHCH_2](\mu\text{-}H)$, **7**. Compounds **5** and **7** are isomers containing substituted η^3-allyl ligands formed by the coupling of the ethylene to the CH-activated β-carbon atom of the acryloyl ligand accompanied by some metal-mediated H-shifts. Compound **6** contains an uncoupled π-coordinated ethylene ligand. Compound **7** was isomerized to **5** thermally at 80 °C. Compound **4** reacts with ethylene in the presence of Me_3NO to yield two new Ru_5 products: $Ru_5(\mu_5\text{-}C)(CO)_{13}[\eta^4\text{-}1{,}1\text{-}\textit{anti}\text{-}\textit{syn}\text{-}[(O_2CMe)C(Me)CHCH_2](\mu\text{-}H)$, **8**, and $Ru_5(\mu_5\text{-}C)(CO)_{13}[\eta^4\text{-}1\text{-}\textit{anti}\text{-}CH(Me)C(O_2CMe)(CH_2)]\text{-}(\mu\text{-}H)$, **9**. Compounds **8** and **9** both contain substituted η^3-allyl ligands formed by the coupling of the ethylene to the CH-activated α-carbon atom of the vinyl acetyl ligand. Compound **8** was isomerized to **9** thermally at 80 °C. All new products were characterized structurally by single-crystal X-ray diffraction analyses.

INTRODUCTION

The coupling of olefins by metal-mediated formation of carbon−carbon bonds is of great interest. The oligomerization of simple olefins like ethylene yields higher-value olefins for use in the synthesis of new polymers, materials, fuels, and chemicals.[1,2] The coupling and polymerization of alkenes with certain polar vinyl monomers (PVMs), such as methyl acrylate and vinyl acetate, yield valuable copolymers such as ethylene−vinyl acetate (EVA).[3,4] Although many of these copolymers are synthesized commercially by using free-radical processes at high temperatures and pressures,[6] it could be advantageous to perform such copolymerizations under milder conditions by using metal-based systems.[3,4] Unfortunately, the development of metal-based olefin copolymerization reactions involving PVMs has been hampered by the basic differences in the reactivities and properties of the different olefins (i.e., insertion/coupling processes) and inhibitory/poisoning effects caused by coordinative properties of oxygen containing functional groups, etc. if they are present.[3a,c,d,f,4a,c,6,7]

In recent studies, we have found that the pentaruthenium cluster complex $Ru_5(\mu_5\text{-}C)(CO)_{15}$, **1**, is able to activate the formyl CH bond in dimethylformamide[8] and in certain aldehydes[9] to form opened Ru_5 cluster complexes containing η^2-C=O bridging acyl ligands, e.g., eq 1.

We also showed that acetylene, HC≡CH, could be coupled to the carbon atom of the bridging formamido ligand in the complex $Ru_5(\mu_5\text{-}C)(CO)_{13}(HNMe_2)(\mu\text{-}\eta^2\text{-}O{=}CNMe_2)(\mu\text{-}H)$ after displacement of the labile Me_2NH ligand to yield the acrylamide complex, $Ru_5(\mu_5\text{-}C)(CO)_{13}[\mu\text{-}\eta^3\text{-}O{=}C\text{-}(NMe_2)CHCH](\mu\text{-}H)$, eq 2.[8]

There are very few examples of the activation of olefinic CH bonds by polynuclear metal complexes.[10,11] It has been proposed that CH activation in olefins proceeds by binuclear mechanisms in polynuclear metal complexes. In the work described herein, we have discovered new examples of CH

Received: February 10, 2019
Published: June 19, 2019

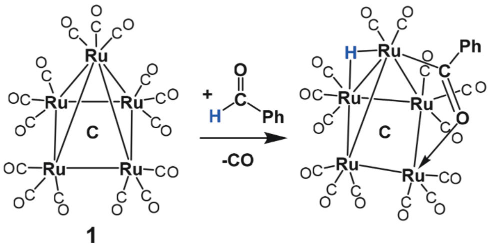

(1)

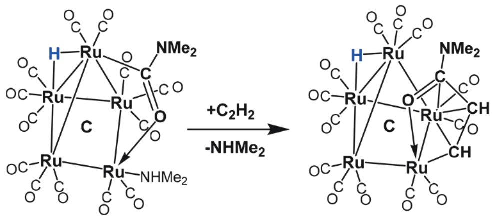

(2)

activation reactions by using the polar olefins methyl acrylate (MA) and vinyl acetate (VAc) and the cluster complex **1**. Most importantly, we have found that the site of CH activation on the vinyl group of the polar olefins changes depending on the nature of the substituent on the vinyl group. We have also investigated the coupling of the metal-activated olefins in these pentaruthenium complexes with ethylene and have found that ethylene can be coupled to the carbon atom at the CH activation site to yield new Ru_5 cluster complexes containing substituted allyl ligands. A preliminary report of this work has been published.[12]

■ RESULTS AND DISCUSSION

Reaction of 1 with Methyl Acrylate, $H_2C{=}C(H)$-CO_2Me. The reaction of compound **1** with methyl acrylate (MA) in benzene solvent at 80 °C over a period of 48 h yielded the new complex $Ru_5(\mu_5\text{-}C)(CO)_{14}[\eta^2\text{-}O{=}C(OMe)\text{-}CH{=}CH](\mu\text{-}H)$, **2** in 35% yield. Compound **2** was characterized by IR, ^1H NMR, and ^{13}C NMR spectroscopy, mass spectrometry, and single-crystal X-ray diffraction analysis. An ORTEP diagram of the molecular structure of **2** is shown in Figure 1. The structure of compound **2** consists of an open cluster of five ruthenium atoms in the form of a "butterfly" cluster of four ruthenium atoms with a carbido ligand C0 in the center with a fifth ruthenium atom Ru4 bridging the wingtips of the Ru_4 cluster. There is a chelating methyl acrylate ligand which has undergone a CH activation at the β-carbon atom C1a that is coordinated to Ru4 and by the ester oxygen atom O1a, Ru4−C1a = 2.054(5) Å, Ru4−O1a = 2.158(5) Å and has thus formed a five-membered metallacyclic ring. There is a double bond between C1a and C2a, C1a−C2a = 1.303(7) Å. The hydrogen atom was transferred to the metal atoms and serves as a bridging hydrido ligand H1, $\delta = -22.18$, across the Ru1−Ru2 bond of the cluster. The two hydrogen atoms remaining on the metalated vinyl group appear as doublets at $\delta = 10.18$, $^3J_{H-H} = 8.0$ Hz, and 6.96, $^3J_{H-H} = 8.0$ Hz, in the H NMR spectrum. The carbon atoms appear at $\delta = 200.94$ (C1a), 124.81 (1 CH C2a), and 181.39 (C3a), and even the carbide carbon atom was observed at 445.67 ppm in the ^{13}C NMR spectrum of **2**, Figure S3.1. The assignments were confirmed by DEPT analysis. Upon metalation, the resonance of C1A was shifted downfield by 70 ppm from 130.2 ppm in the free molecule methyl acrylate to 200.94 ppm in **2**; see Figure S3.2. Komiya et al. reported a structurally similar chelating β-CH-activated methacrylate ligand in the complex $Ru(H)(CH{=}CMeCO_2C_4H_9)(PPh_3)_3$ that was obtained from the reaction of $H_2Ru(PPh_3)_4$ with n-butyl methacrylate many years ago.[13] In the formation of **2**, compound **1** has lost one CO ligand, and one of the Ru−Ru bonds in the cluster was cleaved. The metalated-methyl acrylate ligand in **2** formally serves as a three-electron donor and with 1 electron from the hydrido ligand, 28 electrons from the 14 CO ligands, 4 electrons from the carbido ligand, and 40 electrons from the five metal atoms, the cluster has achieved a total of 76 cluster valence electrons, which is consistent with the bonding models that predict an opened square-pyramidal structure for the cluster; that is, each metal atom formally has an 18 electron configuration.[14]

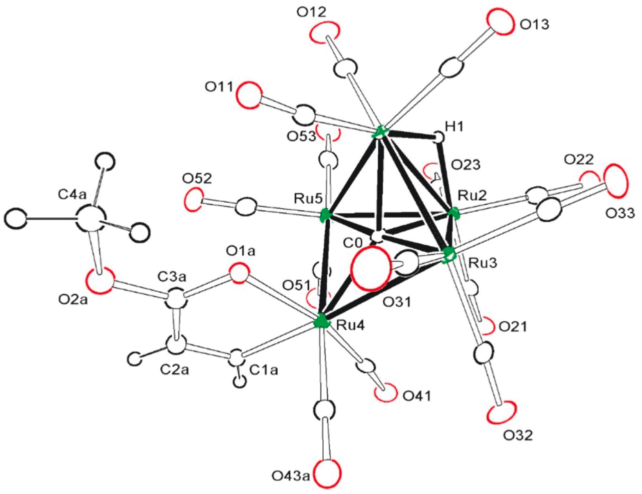

Figure 1. ORTEP diagram of the molecular structure of $Ru_5(\mu_5\text{-}C)(CO)_{14}[\eta^2\text{-}O{=}C(OMe)CH{=}CH](\mu\text{-}H)$, **2**, showing 30% thermal ellipsoid probability. Selected interatomic bond distances (Å) are as follows: Ru1−Ru3 = 2.8405(4), Ru1−Ru5 = 2.8442(4), Ru1−Ru2 = 2.8335(4), Ru2−Ru5 = 2.8550(4) Ru2−Ru3 = 2.8501(4), Ru3−Ru4 = 2.9313(4), Ru4−Ru5 = 2.9388(4), Ru1−H1 = 1.74(3), Ru2−H1 = 1.77(3), Ru4−O1a = 2.158(5), Ru4−C1a = 2.054(5), C1a-C2a = 1.303(7), C2a-C3a = 1.447(6), C3a-O1a = 1.264(6), Ru1−C0 = 2.114(3), Ru2−C0 = 2.119(3), Ru3−C0 = 1.964(3), Ru4−C0 = 2.115(3), Ru5−C0 = 1.959(3).

When a solution of **2** in heptane solvent was heated to reflux (98 °C) for 6 h under a purge of nitrogen, it eliminated one CO ligand and was converted to the product $Ru_5(\mu_5\text{-}C)(CO)_{13}[\mu\text{-}\eta^3\text{-}O{=}C(OMe)CHCH](\mu\text{-}H)$, **3** in 8% yield. Compound **3** was also obtained from **2** in a better yield (24%) by irradiation (visible light only) of solutions of **3** in benzene solvent. Compound **3** was characterized by a combination of IR, ^1H NMR, mass spectrometry, and single-crystal X-ray diffraction analyses. An ORTEP diagram of the molecular structure for compound **3** is shown in Figure 2. The π-bond between the carbon atoms C2 and C3 in **3** is coordinated to Ru3, while C3 is also σ-bonded to Ru4, Ru3−C2 = 2.287(4) Å, Ru3−C3 = 2.205(4) Å, Ru4−C3 = 2.022(4) Å. The ester group is coordinated to Ru4 by its carbonyl oxygen atom O1, Ru4−O1 = 2.182(3) Å. As in **2**, there is a hydrido ligand bridging the "hinge" metal atoms Ru1 and Ru2 of the Ru_4 butterfly portion of the cluster, Ru1−H1 = 1.75(4) Å, Ru2−H1 = 1.76(5) Å, $\delta = -21.02$. Compound **3** is a product of a simple decarbonylation of **2**. With the coordination of the π-bond of the olefinic group, the cluster achieves the required 76 electron count as required for the open square-pyramidal arrangement of the metal atoms of the Ru_5 cluster. Compound

DOI: 10.1021/acs.inorgchem.9b00399
Inorg. Chem. 2019, 58, 8357−8368

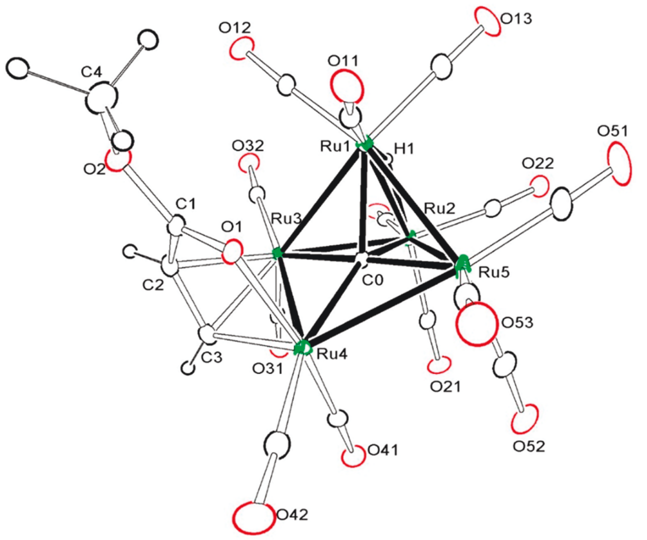

Figure 2. ORTEP diagram of the molecular structure of $Ru_5(\mu_5\text{-}C)(CO)_{13}[\mu\text{-}\eta^3\text{-}O{=}C(OMe)CHCH](\mu\text{-}H)$, **3**, showing 30% thermal ellipsoid probability. Selected interatomic bond distances (Å) are as follows: Ru1−Ru3 = 2.9515(5), Ru1−Ru5 = 2.8441(5), Ru1−Ru2 = 2.8207(5), Ru2−Ru5 = 2.8836(5) Ru2−Ru3 = 2.8265(5), Ru3−Ru4 = 2.7158(5), Ru4−Ru5 = 3.0003(5), Ru1−H1 = 1.75(4), Ru2−H1 = 1.76(5), Ru4−O1 = 2.182(3), Ru4−C3 = 2.022(4), Ru3−C2 = 2.287(4), Ru3−C3 = 2.205(4), C1−C2 = 1.448(6), C2−C3 = 1.419(6), C1−O1 = 1.255(5), Ru1−C0 = 2.114(4), Ru2−C0 = 2.104(4), Ru3−C0 = 1.959(4), Ru4−C0 = 2.086(4), Ru5−C0 = 1.950(4).

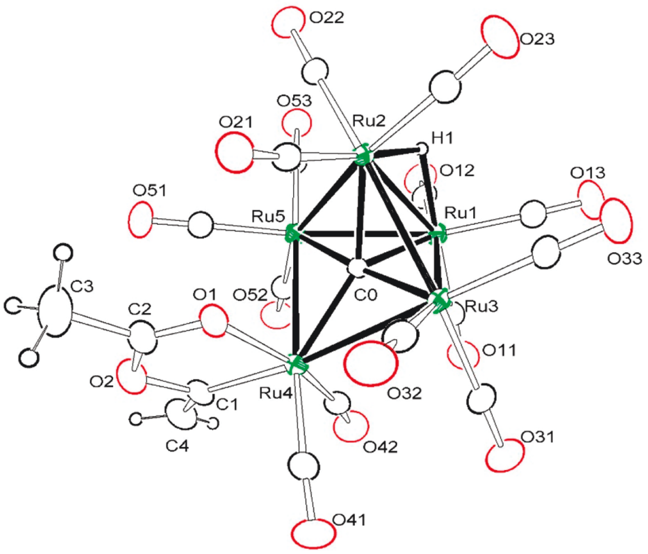

Figure 3. ORTEP diagram of the molecular structure of $Ru_5(\mu_5\text{-}C)(CO)_{14}[\eta^2\text{-}(MeCO_2)C{=}CH_2](\mu\text{-}H)$, **4** showing 25% thermal ellipsoid probability. Selected interatomic bond distances (Å) are as follows: Ru1−Ru3 = 2.8469(4), Ru1−Ru5 = 2.8472(4), Ru1−Ru2 = 2.8412(4), Ru2−Ru5 = 2.8392(4) Ru2−Ru3 = 2.8340(4), Ru3−Ru4 = 2.9436(4), Ru4−Ru5 = 2.9432(6), Ru1−H1 = 1.81(4), Ru2−H1 = 1.71(4), Ru4−O1 = 2.124(3), Ru4−C1 = 2.035(4), C1−C4 = 1.272(6), C1−O2 = 1.486(5), O2−C2 = 1.327(5), C2−O1 = 1.215(5), Ru1−C0 = 2.115(3), Ru2−C0 = 2.118(3), Ru3−C0 = 1.968(3), Ru4−C0 = 2.116(3), Ru5−C0 = 1.955(3).

3 is structurally similar to the compound $Ru_5(\mu_5\text{-}C)(CO)_{13}[\mu\text{-}\eta^2\text{-}O{=}C(NMe_2)CHCH](\mu\text{-}H)$ that was formed from the reaction of $Ru_5(\mu_5\text{-}C)(CO)_{13}(HNMe_2)(\mu\text{-}\eta^2\text{-}O{=}CNMe_2)(\mu\text{-}H)$ with C_2H_2 except that **3** contains an OMe group in the location of the NMe_2 group, see eq 2.[9]

Reaction of 1 with Vinyl Acetate, $H_2C{=}CH(O_2CMe)$. The reaction of **1** with vinyl acetate in a solution in benzene solvent at 80 °C for 42 h yielded the new compound $Ru_5(\mu_5\text{-}C)(CO)_{14}[\eta^2\text{-}(MeCO_2)C{=}CH_2](\mu\text{-}H)$, **4** in 62% yield. Compound **4** was characterized by IR and ^1H NMR spectroscopy, mass spectrometry, and single-crystal X-ray diffraction analyses. An ORTEP diagram of the molecular structure of **4** is shown in Figure 3.

Compound **4** consists of an open cluster of five ruthenium atoms similar to that found in **2**. It also contains a chelating CH-activated vinyl acetate ligand coordinated to the bridging ruthenium atom Ru4 in the form of a five-membered metallacyclic ring. However, unlike **2**, the CH activation that occurred at vinyl group in **4** occurred at the substituted carbon atom C1, Ru4−C1 = 2.035(4) Å, Ru4−O1 = 2.124(3) Å. The C1−C4 bond is a double bond, C1−C4 = 1.272(6) Å. Compound **4** contains one hydrido ligand H1, $\delta = -22.37$, that bridges the Ru1−Ru2 bond. The two hydrogen atoms remaining on the carbon atom C4 appear as doublets at $\delta = 5.65$ ($^3J_{H-H} = 2.4$ Hz) and 5.06 ($^3J_{H-H} = 2.4$ Hz) in the ^1H NMR spectrum. The vinylic carbon atoms C1 and C4 appear at $\delta = 178.83$ (C1) and 106.63 (C4) in the ^{13}C NMR spectrum of **4**, Figure S7.1. The assignments were confirmed by heteronuclear multiple band correlation analysis; see Figure S7.3. Upon metalation, the resonance of C1 was shifted downfield by 37.6 ppm from its position at 141.2 ppm in the free molecule vinyl acetate to 178.8 ppm in **4**; see Figure S7.1.

The reason for the change in the site of CH activation from **2** to **4** may be related to the number of atoms of the acetate substituent that are included in the five-membered metallacyclic ring.[12] In particular, in **4** the acetate group contributes three atoms to the ring; therefore, in order to form a five-membered ring by cyclization, the CH activation must occur at the α-carbon atom of the vinyl group. However, to compare with compound **2**, the C(=O)OMe substituent contributes only two atoms to the metallacyclic ring. Therefore, in order to form a five-membered ring by cyclization with methyl acrylate in **2**, the CH activation must occur at the β-carbon atom of the vinyl group. Efforts to decarbonylate **4** thermally did not yield any stable pentaruthenium carbonyl products containing ligands derived from vinyl acetate.

There are very few structurally characterized examples of metal complexes containing vinyl acetate as a ligand. Deeming et al. reported the complex $Os_3(CO)_{10}[\eta^3\text{-}H_2C{=}CH\text{-}(O_2CMe)]$ a number of years ago, but there were no CH activation reactions in the formation of this compound.[15] We have not been able to find any structurally characterized examples of CH-activated vinyl acetate metal complexes. In order to determine if the site of CH activation in the activated methyl acrylate and vinyl acetate ligands in **2** and **4** has any effect on their reactivity, we investigated the reactions of **2**, **3**, and **4** with ethylene. The coupling of ethylene to methyl acrylate and vinyl acetate is also important to the formation of their valuable copolymers,[4,5]

Reactions of the Ru_5 Complexes with Ethylene. To stimulate these reactions under mild conditions, we used the chemical decarbonylation reagent Me_3NO. The reaction of **2** with ethylene in the presence of Me_3NO at 25 °C yielded three new compounds: $Ru_5(\mu_5\text{-}C)(CO)_{13}[\eta^4\text{-}1\text{-}anti,3\text{-}syn\text{-}\{O{=}C(OMe)\}C(H)C(H)C(H)Me](\mu\text{-}H)$, **5**, $Ru_5(\mu_5\text{-}C)(CO)_{12}$-

$(C_2H_4)[\mu\text{-}\eta^3\text{-}O{=}C(OMe)C(H)C(H)](\mu\text{-}H)$, **6**, and $Ru_5(\mu_5\text{-}C)(CO)_{13}[\eta^4\text{-}anti\text{-}O{=}C(OMe)CH_2CHCHCH_2](\mu\text{-}H)$, **7**, in low yields, 5%, 2%, and 11%, respectively, together with a trace amount of **3** (1% yield). Compounds **5** (7.8% yield) and **6** (6.7% yield) were also obtained from **3** by reaction with ethylene thermally (68 °C) in the absence of Me_3NO. Compound **6** was obtained in a good yield (62%) by reaction of **3** with ethylene in the presence of Me_3NO. All three products were characterized by IR, H NMR, mass spectrum, and single-crystal X-ray diffraction analyses.

An ORTEP diagram of the molecular structure of compound **5** is shown in Figure 4. The structure of **5** contains an open Ru_5C cluster with a hydrido ligand bridging the Ru1−Ru2 bond as found in each of the previous compounds described in this report.

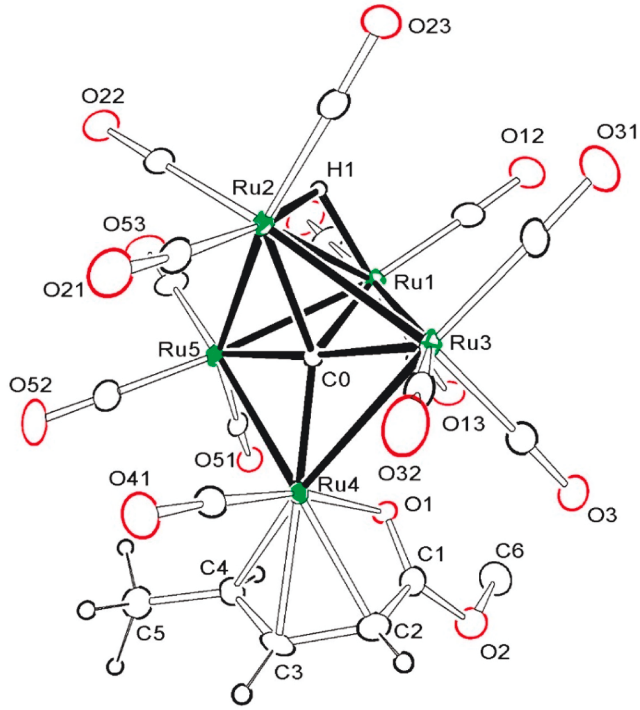

Figure 4. ORTEP diagram of the molecular structure of $Ru_5(\mu_5\text{-}C)(CO)_{13}[\eta^4\text{-}1\text{-}anti,3\text{-}syn\text{-}\{O{=}C(OMe)\}C(H)C(H)C(H)Me](\mu\text{-}H)$, **5**, showing 25% thermal ellipsoid probability. Hydrogen atoms on C6 were omitted for clarity. Selected interatomic bond distances (Å) are as follows: Ru1−Ru2 = 2.8400(7), Ru1−Ru5 = 2.8443(8), Ru1−Ru3 = 2.8585(7), Ru2−Ru5 = 2.8398(7), Ru2−Ru3 = 2.8483(7), Ru3−Ru4 = 2.9289(7), Ru1−H1 = 1.80(2), Ru2−H1 = 1.78(2), Ru4−O1 = 2.239(4), Ru4−C2 = 2.189(7), Ru4−C3 = 2.181(6), Ru4−C4 = 2.223(7), C1−C2 = 1.478(10), C2−C3 = 1.414(11), C3−C4 = 1.410(11), C4−C5 = 1.501(11), C1−O1 = 1.234(8), Ru1−C0 = 2.124(6), Ru1−C0 = 2.124(6), Ru2−C0 = 2.113(5), Ru3−C0 = 1.962(6), Ru4−C0 = 2.046(6), Ru5−C0 = 1.979(6).

The most interesting ligand in **5** is an $\eta^4\text{-}O{=}C(OMe)C(H)C(H)C(H)Me$ "allyl" ligand that is coordinated to the metal atom Ru4 with an *anti*-conformation for the CO_2Me group at atom C2 and a *syn*-conformation for the Me group at C4; see Scheme 1 for the stereochemical definitions of η^3-coordinated allyl ligands.[16]

Scheme 1. Stereochemical Definitions for η^3-Coordinated Allyl Ligands[16]

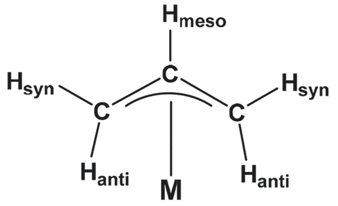

Carbon atoms C2, C3, and C4 form the allyl group and are all coordinated to Ru4, Ru4−C2 = 2.189(7) Å, Ru4−C3 = 2.181(6) Å, Ru4−C4 = 2.223(7) Å. The oxygen atom O1 of the carbonyl of the ester group is also coordinated to Ru4, Ru4−O1 = 2.239(4) Å. The C−C bonding is normal for a η^3-coordinated allyl group: C2−C3 = 1.414(11) Å, C3−C4 = 1.410(11) Å. The two carbon atoms C4 and C5 are derived from a rearranged molecule of ethylene that was coupled to the carbon atom C1a of **2**; see Figure 1. Including the coordinated carbonyl oxygen atom O1, the allyl group serves as a five-electron donor. Thus, compound **5** which contains 13 linear terminal carbonyl ligands has a total of 76 cluster valence electrons for the five metal atoms, which is consistent with an electron-saturated, open square-pyramidal five metal cluster structure.[14]

Compound **6** was also characterized structurally by single-crystal X-ray diffraction analysis. Fortunately, we were also able to synthesize compound **6** independently in 62% yield from the reaction of **3** with C_2H_4 in methylene-d_2 chloride solvent in the presence of Me_3NO at room temperature. An ORTEP diagram of the molecular structure of **6** as found in the solid state is shown in Figure 5. Compound **6** is very interesting because it contains a bridging $\eta^3\text{-}O{=}C(OMe)C(H)C(H)$ acrylate ligand similar to that found in **3**, Ru3−C3 = 2.174(4)

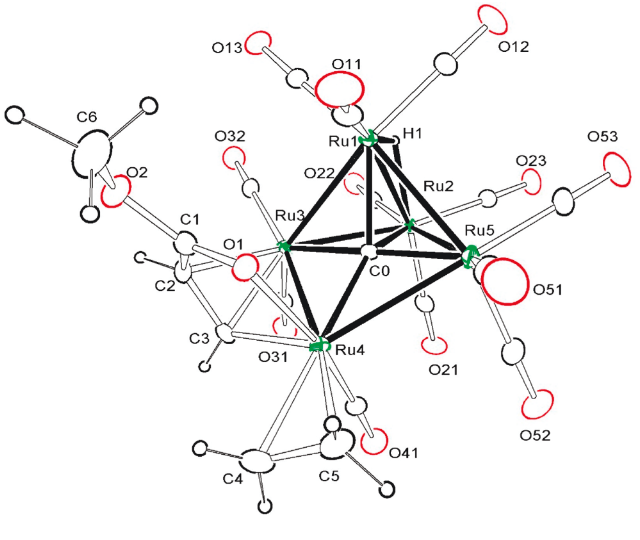

Figure 5. ORTEP diagram of the molecular structure of $Ru_5(\mu_5\text{-}C)(CO)_{12}(C_2H_4)[\mu\text{-}\eta^3\text{-}O{=}C(OMe)C(H)C(H)](\mu\text{-}H)$, **6**, showing 15% thermal ellipsoid probability. Selected interatomic bond distances (Å) are as follows: Ru1−Ru2 = 2.8234(4), Ru1−Ru5 = 2.8459(4), Ru1−Ru3 = 2.9591(4), Ru2−Ru3 = 2.8070(4), Ru2−Ru5 = 2.8731(4), Ru3−Ru4 = 2.7262(4), Ru4−Ru5 = 3.0525(4), Ru1−H1 = 1.72(4), Ru2−H1 = 1.90(4), Ru3−C3 = 2.174(4), Ru3−C2 = 2.268(4), Ru4−C3 = 2.011(4), Ru4−O1 = 2.189(3), Ru4−C4 = 2.224(5), Ru4−C5 = 2.200(4), C1−C2 = 1.447(6), C1−O2 = 1.317(5), C2−C3 = 1.408(6), C1−O1 = 1.233(5), C4−C5 = 1.374(8), Ru1−C0 = 2.111(3), Ru2−C0 = 2.114(3), Ru3−C0 = 1.981(4), Ru4−C0 = 2.087(3), Ru5−C0 = 1.958(4).

DOI: 10.1021/acs.inorgchem.9b00399
Inorg. Chem. 2019, 58, 8357−8368

Å, Ru3−C2 = 2.268(4) Å, Ru4−C3 = 2.011(4) Å, Ru4−O1 = 2.189(3) Å, and also a π-coordinated C_2H_4 ligand on the metal atom Ru4 which is not coupled to the bridging acrylate ligand, Ru4−C4 = 2.224(5) Å, Ru4−C5 = 2.200(4) Å, C1−C2 = 1.447(6) Å. The ^{1}H NMR spectrum of **6** shows only two resonances for the ethylene ligand, δ = 3.48 br and 3.23 m at 21.6 °C. Suspecting dynamical activity, variable temperature ^{1}H NMR measurements were performed, which confirmed that the ethylene ligand is dynamically active at room temperature on the NMR time scale. At −80 °C, separate resonances were observed at δ = 4.86, 3.51, 3.23, and 2.10, for each of the four inequivalent hydrogen atoms on the ethylene ligand. The resonances average in two pairs, 4.86 with 2.10, and 3.51 with 3.23, to give the averaged resonances observed at δ = 3.48 br and 3.43 m at 21.6 °C. At +95 °C, these averaged resonances are observed as two well resolved AA‘BB’ multiplets, as expected, for this ethylene ligand, which is undergoing a rapid 2-fold rotational exchange along the metal−ligand bond axis; see Figure S1 in the Supporting Information. From the coalescence temperature of −60 °C for the resonances at δ = 3.51, 3.23, we were able to calculate the free energy of activation, $\Delta G_{213}^{\dagger}$ = 10.0(3) kcal/mol for the rotational barrier.[17] Other examples of hindered rotation of π-coordinated ethylene about the metal−ligand bond have been observed with similar barriers.[18]

An ORTEP diagram of the molecular structure of compound **7** is shown in Figure 6. The molecule consists of an open Ru_5C cluster with an η^4-O═C(OMe)CH_2CH-CHCH_2 ligand on the metal atom Ru4. It crystallizes in the space group *Cmc*2_1, and the molecule lies on a crystallographic reflection plane. The metal atoms Ru1, Ru2, Ru4, the carbide ligand C0, and the oxygen atom O1 lie on the reflection plane. The η^4-O═C(OMe)CH_2CHCHCH_2 ligand exhibits a 50/50 disorder about this reflection plane. Only one of the two disorder components is shown in Figure 6. The η^4-O═C(OMe)CH_2CHCHCH_2 ligand can be described as a O═C(OMe)CH_2-substituted allyl ligand with the O═C(OMe)-CH_2 group in an *anti*-stereochemistry. The three allyl carbon atoms C3, C4, and C5 and the carbonyl oxygen atom O1 are coordinated to the ruthenium atom Ru4, Ru4−C3 = 2.19(2) Å, Ru4−C4 = 2.186(16) Å, Ru4−C5 = 2.26(2) Å, Ru4−O1 = 2.206(11) Å. There is a hydrido ligand bridging the Ru1−Ru2 bond, Ru1−H12 = 1.73(9), Ru2−H12 = 1.73(9), δ = −22.02.

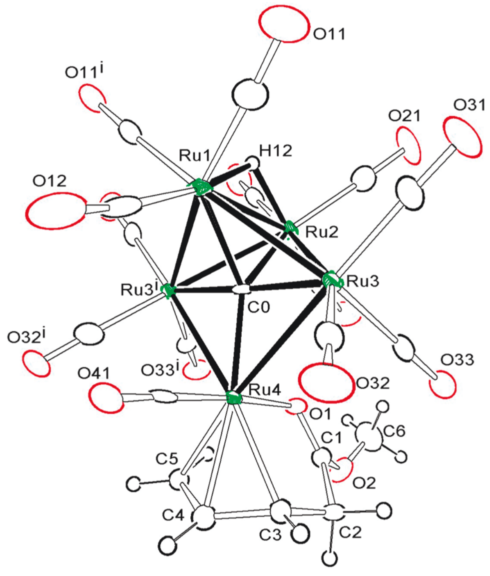

Figure 6. ORTEP diagram of the molecular structure of $Ru_5(\mu_5$-C)$(CO)_{13}[\eta^4$-*anti*-O═C(OMe)CH_2CHCH$CH_2](\mu$-H), **7**, showing 15% thermal ellipsoid probability. Selected interatomic bond distances (Å) are as follows: Ru1−Ru2 = 2.8316(17), Ru1−Ru3 = 2.8680(11), Ru1−Ru3 = 2.8680(11), Ru1−H12 = 1.73(9), Ru2−H12 = 1.73(9), Ru2−Ru3 = 2.8571(12), Ru2−Ru3 = 2.8571(12), Ru3−Ru4 = 2.8975(12), Ru1−C0 = 2.114(13), Ru2−C0 = 2.098(18), Ru3−C0 = 1.9735(7), Ru4−C0 = 2.078(17), Ru4−C3 = 2.19(2), Ru4−C4 = 2.186(16), Ru4−C5 = 2.26(2), Ru4−O1 = 2.206(11).

It would seem like the addition of CO to **6** would lead to **5** or **7**, but unfortunately, all attempts to convert **6** to **5** or **7** by the addition of CO (1 atm) with mild heating in a solution in an NMR tube at 80 °C yielded only compound **2** by elimination of the ethylene ligand and the addition of two equivalents of CO. Thus, although we cannot rule out the formation of **5** or **7** from **6**, it seems unlikely that **6** is an intermediate en route to **5** or **7**. However, some **5** was obtained together with **6** in a thermal reaction of **3** with ethylene at 68 °C in the absence of added CO. Thus, it is possible that **5** could be formed from **3** and ethylene without the need for a CO addition.

On the basis of the above information, a proposed mechanism for the formation of compounds **3**, **5**, **6**, and **7** from reactions of **2** with ethylene in the presence of Me_3NO are presented in Scheme 2. In order to obtain compounds **5** and **7** from **2** or **3**, a molecule of ethylene must be added by C−C bond formation to the CH-activated β-carbon of the acryloyl ligand which is coordinated to Ru4 of the Ru_5 cluster. For the mechanism in Scheme 2, it is assumed that all the important processes occur at the unique bridging metal atom Ru4 of the cluster. For the sake of clarity, the Ru_4C portion of the cluster is not shown in the scheme. Note: the decarbonylation of **2** by irradiation (visible light) yielded compound **3** (24% yield) in the absence of ethylene.

At present, it seems most likely that ethylene is added to **3** or some solvated precursor to **3** derived from the decarbonylation of **2**. This is followed by insertion of the ethylene into the terminal Ru−C bond of the activated methyl acrylate ligand. This would lead to a seven-membered metallacyclic intermediate such as $\mathbf{I_1}$. A CO ligand is then shifted to Ru3 (not shown in the scheme), and this is accompanied β-hydrogen elimination from carbon C3 in either of two ways: (1) β-hydrogen elimination of H1 by pathway (1) would lead to an alkenyl-coordinated hydride intermediate $\mathbf{I_2}$, which could go directly to **5** by coordination of the C_1−C_2 double bond and reductive elimination of the C4−H1 bond to form the methyl group at C4.

(2) Alternatively, a β-hydrogen elimination of H2 from $\mathbf{I_1}$ by pathway (2) would lead to the hydride intermediate $\mathbf{I_3}$. Coordination of the C1−C2 double bond accompanied by the release of the ester group by cleavage of Ru−O bond to the carbonyl oxygen atom would lead to the intermediate $\mathbf{I_4}$, which would then lead to **7** by reductive elimination of the C1−H2 bond upon a recoordination of the carbonyl oxygen atom of the ester group. Note: Compound 7 was converted to **5** by heating a solution in toluene-d_8 solvent to 80 °C for 10 h. At the end of the 10 h period, the ratio of **5**/**7** was 5.60 by ^{1}H NMR integration of the hydride resonances. The **5** to **7** conversion could be achieved mechanistically simply by retracing pathway (2) back to $\mathbf{I_1}$ and then on to **5** by pathway (1). Efforts to obtain **7** from **5** were unsuccessful.

Scheme 2. A Proposed Mechanism for the Addition and Coupling of Ethylene to the Activated Methyl Acrylate Ligand in the Ru_5 Complexes 2 and 3 with the Formation of Compounds 5–7[a]

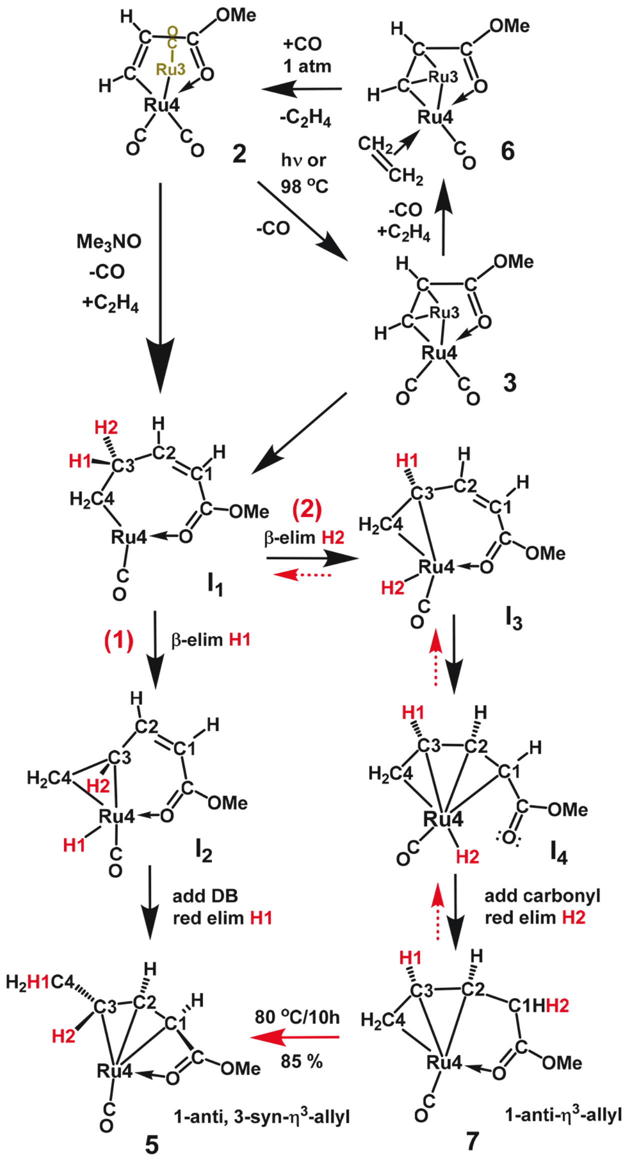

[a] Only ruthenium atoms Ru3 and Ru4 of the cluster that involve the important ligands are shown. Subscripts refer to the number of atoms at a site. Normal case numbers are atom labels. Hydrogen atoms that undergo shifts are colored red.

The reaction of **4** with ethylene in the presence of Me_3NO yielded two products: $Ru_5(\mu_5\text{-}C)(CO)_{13}[\eta^4\text{-}1,1\text{-}anti\text{-}syn\text{-}[(O_2CMe)C(Me)CHCH_2](\mu\text{-}H)$, **8**, and $Ru_5(\mu_5\text{-}C)(CO)_{13}[\eta^4\text{-}1\text{-}anti\text{-}CH(Me)C(O_2CMe)(CH_2)](\mu\text{-}H)$, **9**, in a combined yield of 13%. A small amount of a third product "**X**" ($\delta = -22.43$) that could not be fully characterized due to its very small quantity was detected by H NMR spectroscopy. It was very difficult to separate compounds **8** and **9** by TLC on silica gel. Attempts to purify the mixture by fractional crystallization yielded crystals suitable for single-crystal X-ray diffraction analysis. Interestingly, these crystals contained an undisordered 1:1 mixture of both **8** and **9**, and both structures were established simultaneously at high resolution in a single single-crystal X-ray diffraction analysis. Subsequently, it was discovered that **8** could be isolated from **9** in a pure form by TLC on alumina, but compound **9** was decomposed completely in this alternative workup. However, a small amount of **9** in a pure form was subsequently obtained by TLC on silica gel by a prolonged elution with pure hexane solvent on silica gel. ORTEP diagrams of the molecular structures of **8** and **9** from the analysis of the mixed crystal are shown in Figures 7 and 8, respectively. Compounds **8** and **9** are isomers.

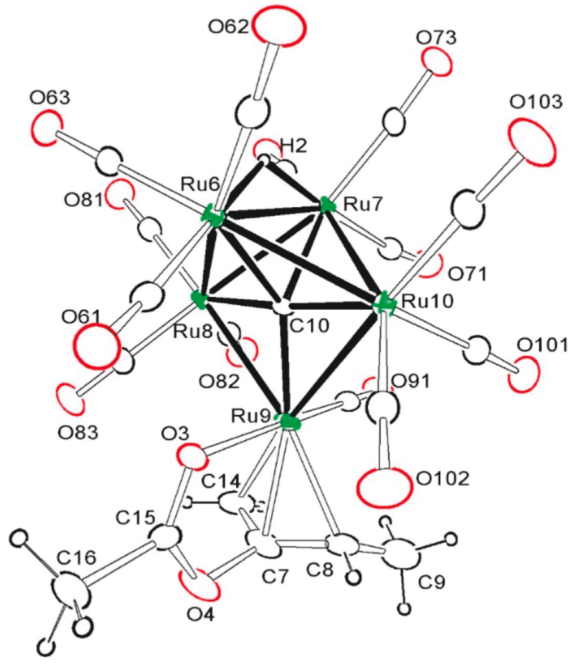

Figure 7. $Ru_5(\mu_5\text{-}C)(CO)_{13}[\eta^4\text{-}1\text{-}anti\text{-}CH(Me)C(O_2CMe)(CH_2)]\text{-}(\mu\text{-}H)$, **8** showing 15% thermal ellipsoid probability. Selected interatomic bond distances (Å) are as follow: Ru6–Ru7 = 2.8251(6), Ru6–Ru8 = 2.8634(6), Ru6–Ru10 = 2.8641(7), Ru7–Ru10 = 2.8595(6), Ru8–Ru9 = 2.8902(7), Ru7–Ru8 = 2.8603(6), Ru6–H2 = 1.63(7), Ru7–H2 = 1.66(7), Ru9–O3 = 2.158(4), Ru9–C7 = 2.163(7), Ru9–C8 = 2.225(8), Ru9–C14 = 2.328(9), Ru9–Ru10 = 2.9067(7), C7–C14 = 1.377(13), C7–C8 = 1.411(14), C7–O4 = 1.449(9), C8–C9 = 1.442(16), C15–O3 = 1.208(7), C15–O4 = 1.275(8), C15–C16 = 1.502(9), Ru6–C10 = 2.131(5), Ru7–C10 = 2.136(5), Ru8–C10 = 1.986(6), Ru9–C10 = 2.034(5), Ru10–C10 = 1.970(6).

Compound **8** contains an open $Ru_5(C)$ cluster with 13 CO ligands and 1 hydrido ligand, $\delta = -22.48$, that bridges the Ru1–Ru2 bond of the cluster. The most interesting ligand in **8** is a disubstituted η^3-allyl ligand, $CH_2C(O_2CMe)C(H)Me$, which contains an acetate substituent at the 2-position C7 and an *anti*-oriented methyl group on the carbon atom C8, Ru9–C7 = 2.163(7) Å, Ru9–C8 = 2.225(8) Å, Ru9–C14 = 2.328(9) Å. The carbonyl group of the acetate substituent is also coordinated the unique metal atom Ru9, Ru9–O3 = 2.158(4) Å. This allyl ligand was formed by a coupling of the ethylene molecule to the CH-activated vinyl acetate ligand in **4** at the α-position; see below.

Compound **9** contains an open Ru_5C cluster similar to that observed in each of the previous compounds in this study. Compound **9** contains 13 CO ligands and one hydrido ligand, $\delta = -22.39$, that bridges the Ru1–Ru2 bond of the cluster. The most interesting ligand in **9** is a disubstituted η^3-allyl

DOI: 10.1021/acs.inorgchem.9b00399
Inorg. Chem. 2019, 58, 8357–8368

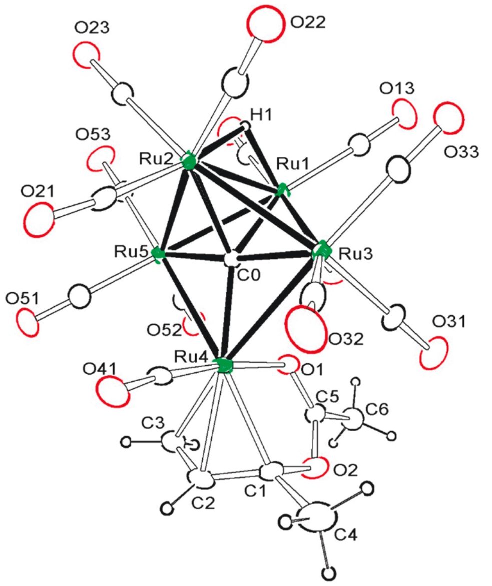

Figure 8. ORTEP diagram of the molecular structure of $Ru_5(\mu_5\text{-}C)(CO)_{13}[\eta^4\text{-}1,1\text{-}\textit{anti-syn}\text{-}[(MeCO_2)C(Me)CHCH_2](\mu\text{-}H)$, **9**, showing 15% thermal ellipsoid probability. Selected interatomic bond distances (Å) are as follows: Ru1−Ru3 = 2.8396(6), Ru1−Ru2 = 2.8440(6), Ru1−Ru5 = 2.8472(7), Ru2−Ru5 = 2.8450(7), Ru2−Ru3 = 2.8495(6), Ru3−Ru4 = 2.9327(7), Ru4−Ru5 = 2.9126(6), Ru1−H1 = 1.74(5), Ru2−H1 = 1.79(5) Ru4−O1 = 2.142(4), Ru4−C1 = 2.152(6), Ru4−C2 = 2.178(6), Ru4−C3 = 2.273(7), C1−C2 = 1.365(10), C1−O2 = 1.465(7), C1−C4 = 1.499(10), C2−C3 = 1.353(10), C5−O1 = 1.230(7), C5−O2 = 1.310(8), Ru1−C0 = 2.141(5), Ru2−C0 = 2.123(6), Ru3−C0 = 1.975(5), Ru4−C0 = 2.048(5), Ru5−C0 = 1.974(5).

ligand, $(MeCO_2)C(Me)CHCH_2$, that is coordinated to the metal atom Ru4, Ru4−C1 = 2.152(6) Å, Ru4−C2 = 2.178(6) Å, Ru4−C3 = 2.273(7) Å. This allyl ligand contains acetate and methyl substituents on the carbon atom C1 in anti and syn-orientations, respectively. The carbonyl group of the acetate substituent is also coordinated to Ru4, Ru4−O1 = 2.142(4) Å.

The allyl ligand in **9** was evidently formed by a coupling of an ethylene molecule to the CH-activated α-carbon atom of vinyl acetate ligand in **4** followed by a hydrogen shift to the CH_2 group to form the methyl group on C1; see the proposed mechanism shown below in Scheme 3. This allyl ligand serves as a five-electron donor to the cluster which obtains a 76 electron configuration that is consistent with the observed open structure for the Ru_5 cluster. Compound **8** appears to be an intermediate in the formation of **9**. In a separate experiment, a sample of pure **8** was transformed to **9** essentially quantitatively by NMR spectroscopy by heating a sample of **8** in an NMR tube in toluene-d_8 solvent at 80 °C for 18 h. Interestingly, the unknown species **X** appeared, hydride resonance at $\delta = -22.43$, and disappeared during the course of this transformation.

A proposed mechanism for the formation of **8** and **9** from **4** is shown in Scheme 3. For this mechanism, it is assumed that all the important processes occur at the unique bridging metal atom of the cluster, i.e., Ru4 in **4**, and for the sake of clarity the Ru_4C portion of the cluster is not shown in the scheme. The reaction is initiated by the removal of a CO ligand from the metal atom Ru4 by reaction with the Me_3NO. This step allows the addition of a molecule of ethylene to a coordination site on that Ru atom in an intermediate such as $\mathbf{I_1}$. Unlike the compound **6** above, the intermediate $\mathbf{I_1}$ was not observed directly. Intermediate $\mathbf{I_1}$ sets the stage for a C−C bond forming insertion-coupling of the ethylene to the CH-activated α-carbon atom of the activated vinyl acetate ligand. Assuming the acetate oxygen atom remains coordinated, this process would lead to the formation of a seven-membered metallacyclic ring in the intermediate shown as $\mathbf{I_2}$. Next, a β-hydrogen elimination transformation from the methylene group at C1 would lead to formation of a coordinated vinyl group with the atoms C1 and C2 and a hydrido ligand in the intermediate $\mathbf{I_3}$. Reductive elimination of a CH bond at C2, which might be induced by coordination of the double bond (**DB**) to C3, would lead to the formation of a methyl group at carbon C2 and would complete the formation of compound **8**.

Compound **8** could be transformed to **9** by a β-hydrogen elimination from the methyl group, carbon C2, in **8** via the intermediate $\mathbf{I_4}$ containing an acetate-substituted butadiene ligand and a hydrido ligand if the Ru4−O bond to the acetate group is temporarily cleaved. Reformation of the Ru−O bond could then induce a reductive elimination and formation of a CH bond and formation of a methyl at C_3 that would yield **9**. The unknown species **X** may be the intermediate $\mathbf{I_4}$ in this reaction series, but we have not been able to confirm this further due to the lack of additional characterization data.

■ CONCLUSIONS

It has been shown that compound **1** reacts with the polar vinyl olefins, methyl acrylate, and vinyl acetate through a cluster opening process that leads to the activation of a CH bond in their vinyl group. By virtue of a preference for the formation of five-membered metallacyclic rings in the complexes, the ester and acetate substituents of methyl acrylate and vinyl acetate produce a directing effect on the site of the CH activation in the vinyl olefin reagents; namely, it occurs at the α-carbon atom for vinyl acetate and the β-carbon atom for methyl acrylate. It was then shown that the CH-activated ligands in these complexes react with ethylene and couple it to the CH-activated carbon atom in the presence of the decarbonylation reagent Me_3NO. This demonstrates an important regiochemical control of the cluster-mediated C−C bond forming process. This coupling ultimately leads to the formation of substituted allyl ligands following some metal-mediated hydrogen shifts.

Substituent-directed CH activation is known to play an important role in stoichiometric and catalytic functionalization of aromatic rings.[19−21] In this work, we have shown that the substitutents on olefins can also play a key role both in the site of CH activation and in the site of their functionalization.

■ EXPERIMENTAL SECTION

General Data. All reactions were performed under an atmosphere of nitrogen. Reagent grade solvents were dried by standard procedure and were freshly distilled prior to use. Infrared spectra were recorded on a Thermo Scientific Nicolet IS10 spectrometer. ^1H NMR spectra were recorded on a Varian Mercury 300 spectrometer operating at 300.1 MHz. Mass spectrometric (MS) measurements were performed by a direct-exposure probe by using electron impact (EI) ionization. $Ru_3(CO)_{12}$ used to make $Ru_5(\mu_5\text{-}C)(CO)_{15}$ was obtained from STREM and was used without further purification. $Ru_5(\mu_5\text{-}C)(CO)_{15}$, **1**, was prepared according to the previously reported procedure.[22] Methyl acrylate, vinyl acetate, and trimethylamine-N-oxide (Me_3NO) were obtained from Sigma-Aldrich and were used without further purification. Product separations were performed by TLC in air on

Scheme 3. A Proposed Mechanism for the Coupling of Ethylene to the Activated Vinyl Acetate Ligand in the Ru_5 Complex 4 and the Formation of Compounds 8 and 9[a]

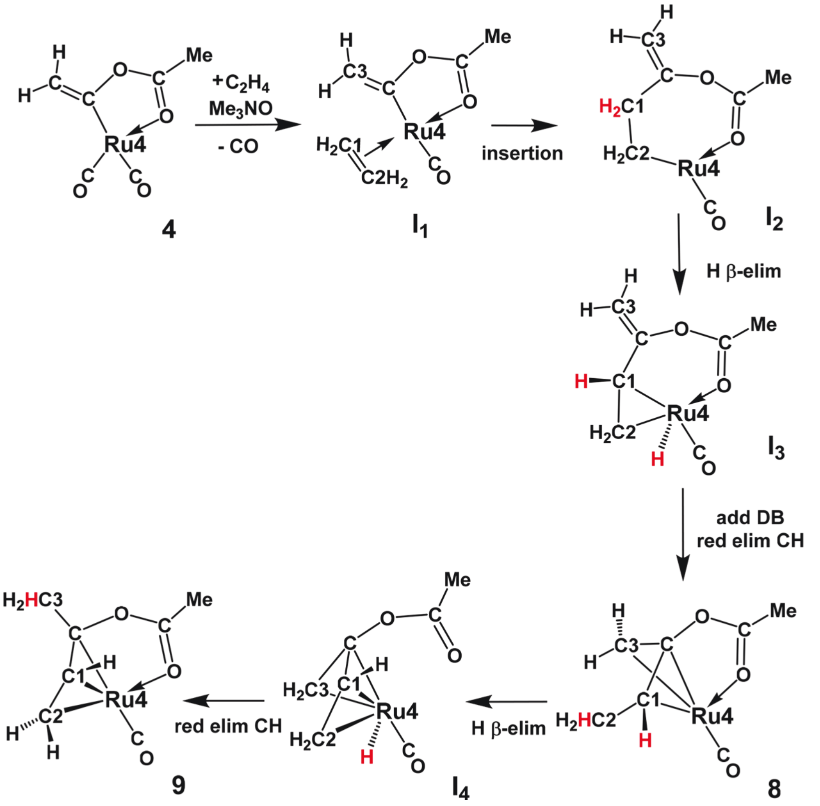

[a]Only the one metal atom Ru4 of the cluster that contains the important ligand transformations is shown. Hydrogen atoms that undergo shifts are colored red.

Analtech 0.25 mm and 0.50 mm silica gel 60 Å F254 or alumina glass plates.

Reaction of 1 with Methyl Acrylate at 80 °C. A 50 mg (0.0529 mmol) amount of **1** was added to a 50 mL three-neck flask in 25 mL of degassed benzene with 1.4 mL of methyl acrylate. After heating for 48 h at 80 °C, the solvent was removed in vacuo, and the product was then isolated by TLC with a hexane/methylene chloride mixture in the order of elution to provide 18.5 mg (35% yield) of yellow $Ru_5(\mu_5\text{-}C)(CO)_{14}[\eta^2\text{-}O{=}C(OCH_3)CH{=}CH](\mu\text{-}H)$, **2**, 1.3 mg (2% yield) of orange $Ru_5(\mu_5\text{-}C)(CO)_{13}[\eta^2\text{-}O{=}C(OCH_3)CH{=}CH](\mu\text{-}H)$, **3**, and 4.1 mg (8% yield) of the known compound black $Ru_5(\mu_5\text{-}C)CO)_{12}(C_6H_6)$.[23] Spectral data for **2**: IR νCO (cm^{-1} in hexane) 2097(w), 2066(s), 2056(s), 2049(s), 2036(w), 2022(m), 2018(sh), 2014(sh), 1995(sh), 1991(m), 1976(w). ^1H NMR (CD_2Cl_2, in ppm) δ = 10.18 (d, 8 Hz, 1H, Ru−C(H)=C(H)-C), 6.96 (d, 8 Hz, 1H, Ru−C(H)=C(H)-C), 3.65 (s, 3H, O = $COCH_3$), −22.18 (s, 1H, hydride). ^{13}C NMR (CD_2Cl_2, 100.66 MHz, δ in ppm): 445.67 (1 C carbide), 200.94 (1 CH C1a), 198.39 (CO), 197.64 (CO), 197.10 (CO), 193.14 (CO), 192.54 (CO), 192.45 (CO), 191.89 (CO), 191.43 (CO), 181.39 (C3a), 124.81 (1 CH C2a), 54.63 (1 CH_3). EI/MS *m*/*z*. M+ = 995.5. The isotope distribution pattern is consistent with the presence of five ruthenium atoms. Spectral data for **3**: IR νCO (cm^{-1} in hexane) 2094(w), 2064(s), 2056(w), 2048(vs), 2038(s), 2026(w), 2017(w), 2002(vw), 1989(w), 1970(vw). ^1H NMR (CD_2Cl_2, in ppm) δ = 10.59 (d, $^3J_{H-H}$ = 5 Hz, 1H, Ru−C(**H**)=C(H)-C), 4.57 (d, $^3J_{H-H}$ = 5 Hz, 1H, Ru−C(H)=C(**H**)−C), 3.55 (s, 3H, OMe), 2.77, −21.02 (s, 1H, hydride). EI/MS *m*/*z*. 967.5. The isotope distribution is consistent with the presence of five ruthenium atoms.

Deacarbonylation of 2 at 98 °C. A 12.7 mg (0.013 mmol) amount of **2** was added to a 50 mL three-neck flask in 20 mL of degassed heptane. After heating for 6 h at 98 °C, the solvent was removed in vacuo, and the products were then isolated by TLC with a hexane/methylene chloride solvent mixture to provide in order of elution: 1.1 mg of starting material of **2**, and 1.0 mg (8% yield) of $Ru_5(\mu_5\text{-}C)(CO)_{13}[\mu\text{-}\eta^3\text{-}O{=}C(OMe)CHCH](\mu\text{-}H)$, **3**. The presence of significant amounts of **1** was observed in the FTIR spectra of the reaction mixture, but the exact amount could not be quantitatively determined because it decomposes readily during the TLC isolation of the product **3**.

Decarbonylation of 2 to 3 by Irradiation. A 16.0 mg (0.016 mmol) amount of **2** was added to a 50 mL three-neck flask in 20 mL of degassed benzene. A slow purge of nitrogen was passed through the solution by using a rubber septum with a pipet. The solution was irradiated (visible light only) by using a tungsten lamp positioned approximately 5 cm from the flask while nitrogen was passed through the solution. The solution developed an orange color. After the solution was irradiated for 10.5 h, the tungsten lamp was removed, the solvent was removed in vacuo, and the compounds were then separated by TLC with a hexane/methylene chloride solvent mixture to provide in order of elution: 2.6 mg of starting material, **2**, and 3.7 mg (24% yield) of **3**, and 1.1 mg of a benzene adduct of $Ru_5(\mu_5\text{-}C)(CO)_{15}$, $Ru_5(\mu_5\text{-}C)(CO)_{12}(\eta^6\text{-}C_6H_6)$.[23]

Synthesis of $Ru_5(\mu_5\text{-}C)(CO)_{14}[\eta^2\text{-}(MeCO_2)C{=}CH_2](\mu\text{-}H)$, 4 from 1 and Vinyl Acetate at 80 °C. A 50.6 mg (0.054 mmol) amount of **1** was added to a 50 mL three-neck flask in 25 mL of degassed benzene with 350 μL of vinyl acetate. After heating for 42 h at 80 °C, the solvent was removed in vacuo, and the product was then isolated by TLC with a hexane/methylene chloride solvent mixture to provide 33.2 mg (62% yield) of $Ru_5(\mu_5\text{-}C)(CO)_{14}[\eta^2\text{-}(MeCO_2)C{=}CH_2](\mu\text{-}H)$, **4**. Spectral data for **4**: IR νCO (cm^{-1} in hexane) 2097(w), 2066(s), 2057(vs), 2050(m), 2036(w), 2023(sh), 2019(w), 2013(sh), 1996(w), 1990(w), 1986(sh), 1980(vw). ^1H NMR (CD_2Cl_2, in ppm) δ = 5.65 (d, $^3J_{H-H}$ = 2.4 Hz, 1H, Ru−C=$\mathbf{CH_2}$), 5.06 (d, $^3J_{H-H}$ = 2.4 Hz, 1H, Ru−C=$\mathbf{CH_2}$), 2.09 (s, 3H, O=C(Me)), −22.37 (s, 1H, hydride). ^{13}C NMR (CD_2Cl_2, 100.66 MHz,

δ in ppm): 197.70 (CO), 196.84 (CO), 194.86 (CO), 194.79 (CO), 192.89 (CO), 192.67 (CO), 192.19 (CO), 191.48 (CO), 191.29 (CO), 181.95 (C2), 178.83 (C1), 106.63 (1 CH_2), 18.28 (1 CH_3). EI/MS *m*/*z*. M^+ = 995.5. The isotope distribution pattern is consistent with the presence of five ruthenium atoms.

Reaction of 2 with Ethylene in the Presence of Trimethylamine N-Oxide at 25 °C. A 41.9 mg (0.042 mmol) amount of **2** was added to a 50 mL three-neck flask in 20 mL of degassed hexane. A slow purge of ethylene gas at 1 atm was passed through the solution for 10 min. Then 16.4 mg (0.22 mmol) of Me_3NO was added to the solution, while the purge with ethylene gas was continued. After stirring for 8 h at room temperature (25 °C) with the slow purge of ethylene, the solvent was removed in vacuo, and the products were then isolated by TLC with a hexane/methylene chloride solvent mixture to provide in order of elution: 0.8 mg of starting material, **2**, 0.4 mg (1% yield) of **3**, 2.1 mg (5% yield) of $Ru_5(\mu_5\text{-C})(CO)_{13}[\eta^4\text{-}$*anti,syn*-O=C(OMe)C(H)C(H)C(H)Me](μ-H), **5**, 0.8 mg (2% yield) of $Ru_5(\mu_5\text{-C})(CO)_{12}(C_2H_4)[\mu\text{-}\eta^3\text{-}$O=C(OMe)C(H)C(H)]($\mu$-H), **6**, and 4.7 mg (11% yield) of $Ru_5(\mu_5\text{-C})(CO)_{13}[\eta^4\text{-}$*anti*-O=C(OMe)$CH_2$CHCH$CH_2$]($\mu$-H), **7**. Spectral data for **5**: IR νCO (cm^{-1} in hexane) 2088(w), 2058(s), 2048(vs), 2034(w), 2017(m), 2001(w), 1990(vw), 1976(w), 1965(w). ^1H NMR (CD_2Cl_2, in ppm) δ = 5.35 (d, $^3J_{H-H}$ = 7.5 Hz, 1H, C−C(**H**)−C(H)), 4.97 (dd, $^3J_{H-H}$ = 6.9 Hz, $^3J_{H-H}$ = 11.1 Hz 1H, C−C(H)−C(**H**)-C(H)), 3.46 (dq, $^3J_{H-H}$ = 6.0 Hz, $^3J_{H-H}$ = 12.0 Hz, 1H, C(H)−C(**H**)-C(H_3)), 3.39 (s, 3H, O**Me**), 2.39 (d, $^3J_{H-H}$ = 6.0 Hz, 3H, C(H)−C(H)−C(**H_3**)) −22.46 (s, 1H, hydride). EI/MS *m*/*z*. 996. The isotope distribution is consistent with the presence of five ruthenium atoms. Spectral data for **6**: IR νCO (cm^{-1} in hexane) 2090(m), 2063(s), 2046(vs), 2028(m) 2024(m), 2012(w), 2001(vw), 1994(w), 1982(w), 1959(vw). ^1H NMR ($C_6D_5CD_3$ at 95 °C, in ppm) δ = 10.70 (d, $^3J_{H-H}$ = 5.4 Hz, 1H, Ru−C(**H**)-C(H)−C(OMe)), 4.07 (d, $^3J_{H-H}$ = 5.4 Hz, 1H, Ru−C(H)=C(**H**)-C(OMe)), 3.53 (m, 2H, C_2H_4), 3.41 (m, 2H, C_2H_4), 2.82 (s, 3H, **OMe**), −20.86 (s, IH, hydride). ^1H NMR ($C_6D_5CD_3$ at −80 °C, in ppm) δ = 10.39 (d, $^3J_{H-H}$ = 4.4 Hz, 1H, Ru−C(**H**)−C(H)−C(OMe)), 4.86 (b, 1H, C_2H_4), 3.76 (b, 1H, Ru−C(H)=C(**H**)-C(OMe)), 3.50 (b, 1H, C_2H_4), 3.22 (b, 1H, C_2H_4), 2.38 (s, 3H, **OMe**), 2.1 (b, 1H, C_2H_4), −21.17 (s, IH, hydride). EI/MS *m*/*z*. 996. The isotope distribution is consistent with the presence of five ruthenium atoms. Spectral data for **7**: IR νCO (cm^{-1} in hexane) 2088(w), 2058(s), 2048(vs), 2034(w) 2017(m), 2001(w), 1990(vw), 1976(w), 1965(w). ^1H NMR (C_6D_6, in ppm) δ = 4.48 (dd, $^3J_{H-H}$ = 8.0 Hz, $^3J_{H-H}$ = 8.0 Hz, 1H, C(OMe)-C(H_2)-C(**H**)-C(H)), 4.44 (dd, $^2J_{H-H}$ = 2.4 Hz, $^3J_{H-H}$ = 8.0 Hz, 1H, C(OMe)-C(H_2)-C(H)−C(H)−C(**H_2**)), 3.88 (ddd, $^3J_{H-H}$ = 13.2 Hz, $^3J_{H-H}$ = 8.0 Hz, $^3J_{H-H}$ = 8.0 Hz 1H, C(OMe)-C(H_2)-C(H)−C(**H**)-C(H_2)), 2.60 (dd, $^3J_{H-H}$ = 8.0 Hz, $^2J_{H-H}$ = 20.4 Hz, 1H, C(OMe)-C(**H_2**)-C(H)−C(H)−C(H_2)), 1.71 (d, $^2J_{H-H}$ = 20.4 Hz, 1H, C(OMe)-C(**H_2**)-C(H)−C(H)−C(H_2)), 1.59 (dd, $^3J_{H-H}$ = 13.2 Hz, $^2J_{H-H}$ = 2.4 Hz, 1H, C(OMe)-C(H_2)-C(H)−C(H)−C(**H_2**)), −22.02 (s, 1H, hydride). EI/MS *m*/*z*. 996. The isotope distribution is consistent with the presence of five ruthenium atoms.

Reaction of 3 with Ethylene in the Presence of Me_3NO. 12.2 mg (0.013 mmol) of **3** was dissolved in 3.0 mL of methylene chloride-d_2 in a small, 10 mL one-neck flask with a side arm. A slow purge of C_2H_4 at 1 atm was passed through the solution for 10 min followed by an addition of 1.5 mg (0.020 mmol) of Me_3NO to the solution. The solution was allowed to stir at room temperature, while the slow purge of C_2H_4 continued. An ^1H NMR spectrum was recorded after 5 h reaction and revealed the formation of compound **6**. Another addition of Me_3NO equaling 1.3 mg (0.017 mmol) was added to the solution, and the purge with C_2H_4 was continued. A final ^1H NMR was taken after 15 h reaction time which showed compound **6** as the major product The solvent was then removed by a fast stream of N_2, and the products were then isolated by TLC with a hexane/methylene chloride solvent mixture to provide in order of elution: 2.1 mg of unreacted **3** and 7.6 mg (62% yield) of compound **6**.

Thermal Reaction of 3 and Ethylene at 68 °C. Fifteen mg (0.0155 mmol) of **3** was added to a 50 mLthree neck flask in 10 mL of degassed hexane. A slow purge of ethylene was passed through the solution by using a rubber septum. After refluxing for 48 h, the solvent was removed in vacuo, and the products were isolated by TLC using pure hexane in the order of elution: 3.2 mg (21%) of **2**, 1.2 mg of unreacted **3**, 1.0 mg (6.7%) of **6**, and 1.2 mg (7.8%) of **5**.

Reaction of 6 with CO at 75 °C. 7.6 mg (0.0078 mmol) of **6** was dissolved in 1.5 mL of toluene-d_8 in an NMR tube. CO was slowly purged through the solution for 2 min. The solution was then heated to 75 °C in a constant temperature bath for 22 h. ^1H NMR spectra showed the gradual formation of compound **2** during this period. TLC workup of this solution at the end of the period using pure hexane provided 1.5 mg (19% yield) of **2**.

Isomerization of 7 to 5 at 80 °C. 4.2 mg (0.004 mmol) of **7** was dissolved in 1.5 mL of toluene-d_8 in an NMR tube. The solution was then heated to 80 °C in a constant temperature oil bath for 10 h. ^1H NMR spectra were recorded intermittently during this period. These spectra showed a slow conversion of **7** to **5**. At the end of the 10 h period, the ratio of the two isomers based on integration of the hydride peaks was 5.60 for compound **5** to 1.00 for compound **7**. Similar efforts to convert **5** to **7** yielded no **7** at all.

Reaction of 4 with Trimethylamine N-Oxide and Ethylene at 25 °C. 43.0 mg (0.043 mmol) of **4** was added to a 50 mL three-neck flask in 25 mL of degassed hexane at 25 °C. A slow purge of ethylene gas at 1 atm was passed through the solution for 10 min. Then 10.0 mg (0.13 mmol) of Me_3NO was added to the hexane solution. After stirring for 6 h at 25 °C under a slow purge of ethylene, the solvent was then removed in vacuo. Separation by TLC in silica gel with a hexane/methylene chloride solvent mixture yielded a single yellow band containing 16.2 mg of a mixture (3:7 ratio of **8** to **9** by ^1H NMR) of two compounds: $Ru_5(\mu_5\text{-C})(CO)_{13}[\eta^4\text{-}$*anti*-($O_2$CMe)-C($CH_2$)CHCMe]($\mu$-H), **8**, and $Ru_5(\mu_5\text{-C})(CO)_{13}[\eta^4\text{-}$1,1-*syn-anti*-[($O_2$CMe)C(Me)CH$CH_2$]($\mu$-H), **9**. There was also an unknown trace product **X** that could not be isolated or fully characterized, but its presence was observed in the form of a metal hydride resonance at δ = −22.43 in toluene-d_8 solvent. Crystals were obtained from solutions of this mixture of **8** and **9** and were found to contain a 1:1 combination of **8** and **9**. These crystals were successfully analyzed by single-crystal X-ray diffraction analysis; see below. Subsequently, efforts to obtain **8** and **9** in pure forms were successful based on the following procedures. The mixture of **8** and **9** was separated on a SiO_2 TLC plate that had been dried in an oven (110 °C for 24 h) with elution by using pure hexane solvent to yield first 1.0 mg (2% yield) of pure yellow **8** followed by a yellow band that contained a mixture of the two isomers of **8** and **9** 5.8 mg (13% yield). Compound **9** was subsequently isolated in a pure form by further TLC treatment of the remaining mixture of isomers on Al_2O_3 but the compound **8**, and the traces of **X** that was in this sample were lost due to decomposition on this support. Spectral data for **8**: IR νCO (cm^{-1} in hexane) 2089(w), 2059(s), 2048(vs), 2034(w) 2018(m), 2003(w), 1991(vw), 1984(vw), 1975(w). ^1H NMR (CD_2Cl_2, in ppm) δ = 5.15 (dq, $^3J_{H-H}$ = 6.6 Hz, $^4J_{H-H}$ = 2.4 Hz, 1H, Ru−C(**H**)-CMe), 4.52 (dd, $^3J_{H-H}$ = 5.4 Hz, $^4J_{H-H}$ = 2.4 Hz, 1H, Ru−C(**H_2**)-C), 3.31 (d, $^3J_{H-H}$ = 5.4 Hz, 1H, Ru−C(**H_2**)-C), 1.72 (s, 3H, O_2C**Me**), 1.55 (d, $^3J_{H-H}$ = 6.9 Hz, 1H, Ru−C(H)-C**Me**), −22.478 (s, 1H, hydride). EI/MS *m*/*z* M^+ = 995.5. The isotope distribution is consistent with the presence of five ruthenium atoms. Spectral data for **9**: IR νCO (cm^{-1} in hexane): 2089(w), 2060(s), 2049(vs), 2035(w) 2019(m), 2005(w), 1991(vw), 1981(w), 1968(w). ^1H NMR (CD_2Cl_2, in ppm): δ = 4.88 (dd, $^2J_{H-H}$ = 2.7 Hz, $^3J_{H-H}$ = 8.4 Hz, 1H, Ru−C(**H_2**)-C(H)-C), 4.16 (dd, $^3J_{H-H}$ = 8.4 Hz, $^3J_{H-H}$ = 13.2 Hz 1H, Ru−C(H_2)-C(**H**)-C), 2.79 (s, 3H, O_2C**Me**), 2.18 (dd, $^2J_{H-H}$ = 2.7 Hz, $^3J_{H-H}$ = 13.2 Hz, 1H, Ru−C(**H_2**)-C(H)-C), 1.77 (s, 3H, C(H)−C(C-**Me**)-O −22.39 (s, 1H, hydride). EI/MS *m*/*z* M^+ = 995.5. The isotope distribution is consistent with the presence of five ruthenium atoms.

Isomerization of 8 to 9 at 80 °C. 0.8 mg (0.001 mmol) of **8** was dissolved in 1.5 mL of toluene-d_8 in an NMR tube. The solution was then heated to 80 °C in a constant temperature silicone oil bath for 18 h. ^1H NMR spectra were recorded intermittently during this period. These spectra showed a slow conversion of **8** to **9**. During this period, formation and subsequent disappearance of small, but significant quantities, of the unknown compound **X** were observed at δ = −22.43

during the course of the transformation. Note: the hydride resonances for **8** and **9** appear at $\delta = -22.36$ and $\delta = -22.29$, respectively, in toluene-d_8 solvent. At the end of the 18 h period, the conversion of **8** to **9** was complete (100%) as determined by ^{1}H NMR spectroscopy. No **X** remained in the sample.

Crystallographic Analyses. Single crystals of compounds **2**−**9** suitable for X-ray diffraction analyses were obtained by slow evaporation of solvent from solutions of the pure compounds at room temperature. Note: compounds **8** and **9** were cocrystallized in the same crystalline form. X-ray intensity data were measured by using a Bruker D8 QUEST diffractometer equipped with a PHOTON-100 CMOS area detector and an Incoatec microfocus source (Mo Kα radiation, $\lambda = 0.71073$ Å).[24] Full details for these analyses are available in the Supporting Information. Crystal data, data collection parameters, and results for each analysis are summarized in Table S1, Supporting Information.

■ ASSOCIATED CONTENT

Ⓢ Supporting Information

The Supporting Information is available free of charge on the ACS Publications website at DOI: 10.1021/acs.inorgchem.9b00399.

Details of the syntheses and characterizations of the new compounds (PDF)

Accession Codes

CCDC 1865326−1865330 (for **3**, **5**, **6**, **7**, and **8** and **9** (combined)) and 1840850 and 1840851 (for **2** and **4**) contain the supplementary crystallographic data for this paper. These data can be obtained free of charge via www.ccdc.cam.ac.uk/data_request/cif, or by emailing data_request@ccdc.cam.ac.uk, or by contacting The Cambridge Crystallographic Data Centre, 12 Union Road, Cambridge CB2 1EZ, UK; fax: +44 1223 336033.

■ AUTHOR INFORMATION

Corresponding Author

*E-mail: Adamsrd@mailbox.sc.edu.

ORCID

Richard D. Adams: 0000-0003-2596-5100

Notes

The authors declare no competing financial interest.

■ ACKNOWLEDGMENTS

This research was supported by Grant 1764192 from the National Science Foundation. The authors thank Dr. Greg Morrison for collection of the diffraction data for compound **6** and Dr. Perry Pellechia for recording the ^{13}C NMR spectra for compounds **2** and **4** and variable temperature ^{1}H NMR spectra for compound **6**.

■ REFERENCES

(1) (a) Sydora, S. Selective Olefin Oligomerization. *Organometallics* **2019**, *38*, 997−1010. (b) Parshall, G. W.; Ittel, S. D. *In Homogeneous Catalysis. The Applications and Chemistry of Catalysis by Soluble Transition Metal Complexes*; Wiley-Interscience: New York, 1992, Ch. 4. (c) Collman, J. P.; Hegedus, L. S.; Norton, J. R.; Finke, R. G. *In Principles and Applications of Organotransition Metal Chemistry*; University Science Books: Mill Valley, CA, 1987, Ch. *11*. (d) Stürzel, M.; Mihan, S.; Mülhaupt, R. From Multisite Polymerization Catalysis to Sustainable Materials and All-Polyolefin Composites. *Chem. Rev.* **2016**, *116*, 1398−1433. (e) Baier, M. C.; Zuideveld, M. A.; Mecking, S. Post-Metallocenesinthe Industrial Production of Polyolefins. *Angew. Chem., Int. Ed.* **2014**, *53* (37), 9722−9744. (f) Sinn, H.; Kaminsky, W. Ziegler-Natta Catalysis. *Adv. Organomet. Chem.* **1980**, *18*, 99−149. (g) Kaminsky, W. Discovery of Methylaluminoxane as Cocatalyst for Olefin Polymerization. *Macromolecules* **2012**, *45* (8), 3289−3297. (h) Cossee, P. Ziegler-Natta Catalysis I. Mechanism of Polymerization of C-Olefins with Ziegler-Natta Catalysts. *J. Catal.* **1964**, *3*, 80−88.

(2) (a) Ittel, S. D.; Johnson, L. K.; Brookhart, M. Late-Metal Catalysts for Ethylene Homo- and Copolymerization. *Chem. Rev.* **2000**, *100*, 1169−1204. (b) Gibson, V. C.; Spitzmesser, S. K. Advances in Non-Metallocene Olefin Polymerization Catalysis. *Chem. Rev.* **2003**, *103*, 283−315. (c) McKnight, A. L.; Waymouth, R. M. Group 4 *ansa*-cyclopentadienyl-amido catalysts for olefinpolymerization. *Chem. Rev.* **1998**, *98*, 2587−2598. (d) Coates, G. W. Precise control of polyolefin stereochemistry using single-site metal catalysts. *Chem. Rev.* **2000**, *100*, 1223−1252. (e) Kaminsky, W.; Laban, A. Metallocene Catalysis. *Appl. Catal., A* **2001**, *222*, 47−61. (f) Sinn, H.; Kaminsky, W. Ziegler-Natta Catalysis. *Adv. Organomet. Chem.* **1980**, *18*, 99−149. (g) Cossee, P. Ziegler-Natta Catalysis I. Mechanism of Polymerization of -Olefins with Ziegler-Natta Catalysts. *J. Catal.* **1964**, *3*, 80−88. (h) Mecking, S. Cationic nickel and palladium complexes with bidentate ligands for the C-C linkage of olefins. *Coord. Chem. Rev.* **2000**, *203*, 325−351. (i) Klosin, J.; Fontaine, P. P.; Figueroa, R. Development of Group IV Molecular Catalysts for High Temperature Ethylene-α-Olefin Copolymerization, Reactions. *Acc. Chem. Res.* **2015**, *48* (7), 2004−2016. (j) Gates, D. P.; Svejda, S. A.; Onate, E.; Killian, C. M.; Johnson, L. K.; White, P. S.; Brookhart, M. Synthesis of Branched Polyethylene Using (R-Diimine)nickel(II) Catalysts: Influence of Temperature, Ethylene Pressure, and Ligand Structure on Polymer Properties. *Macromolecules* **2000**, *33*, 2320−2334. (k) Wang, J.; Zhang, N.; Li, C. Q.; Shi, W. G.; Lin, Z. Y. Nickel complexes based on hyperbranched salicylaldimine ligands: Synthesis, characterization, and catalytic properties for ethylene Oligomerization. *J. Organomet. Chem.* **2016**, *822*, 104−111. (l) Wang, S.; Sun, W.-H.; Redshaw, C. Recent progress on nickel-based systems for ethylene oligo-/polymerization catalysis. *J. Organomet. Chem.* **2014**, *751*, 717−741. (m) Keim, W. Oligomerization of Ethylene to a-Olefins: Discovery and Development of the Shell Higher Olefin Process (SHOP). *Angew. Chem., Int. Ed.* **2013**, *52*, 12492−12496. (n) Nicholas, C. P. Applications of light olefin oligomerization to the production of fuels and chemicals. *Appl. Catal., A* **2017**, *543*, 82−97.

(3) (a) Chen, Z.; Brookhart, M. Exploring Ethylene/Polar Vinyl Monomer Copolymerizations Using Ni and Pd α-Diimine Catalysts. *Acc. Chem. Res.* **2018**, *51*, 1831−1839. (b) Zhang, Y.; Mu, H.; Pan, L.; Wang, X.; Li, Y. Robust Bulky [P,O] Neutral Nickel Catalysts for Copolymerization of Ethylene with Polar Vinyl Monomers. *ACS Catal.* **2018**, *8*, 5963−5976. (c) Navarro, M.; Rosar, V.; Montini, T.; Milani, B.; Albrecht, M. Olefin Dimerization and Isomerization Catalyzed by Pyridylidene Amide Palladium Complexes. *Organometallics* **2018**, *37*, 3619−3630. (d) Nakamura, A.; Anselment, T. M. J.; Claverie, J.; Goodall, B.; Jordan, R. F.; Mecking, S.; Rieger, B.; Sen, A.; van Leeuwen, P. W. N. M.; Nozaki, K. Ortho-Phosphinobenzenesulfonate: A Superb Ligand for Palladium-Catalyzed Coordination-Insertion Copolymerization of Polar Vinyl Monomers. *Acc. Chem. Res.* **2013**, *46*, 1438−1449. (e) Sui, X.; Dai, S.; Chen, C. Ethylene Polymerization and Copolymerization with Polar Monomers by Cationic Phosphine Phosphonic Amide Palladium Complexes. *ACS Catal.* **2015**, *5*, 5932−5937. (f) Guironnet, D.; Roesle, P.; Rünzi, T.; Göttker-Schnetmann, I.; Mecking, S. Insertion Polymerization of Acrylate. *J. Am. Chem. Soc.* **2009**, *131*, 422−423. (g) Mecking, S.; Johnson, L. K.; Wang, L.; Brookhart, M. Mechanistic Studies of the Palladium-Catalyzed Copolymerization of Ethylene and)-Olefins with Methyl Acrylate. *J. Am. Chem. Soc.* **1998**, *120*, 888−899. (h) Drent, E.; van Dijk, R.; van Ginkel, R.; van Oort, B.; Pugh, R. I. Palladium catalysedcopolymerisation of ethene with alkylacrylates: polar comonomerbuilt into the linear polymer chain. *Chem. Commun.* **2002**, 744−745. (i) Skupov, K. M.; Marella, P. R.; Simard, M.; Yap, G. P. A.; Allen, N.; Conner, D.; Goodall, B. L.; Claverie, J. P. Palladium Aryl Sulfonate Phosphine Catalysts for the Copolymerization of Acrylates with Ethene. *Macromol. Rapid Commun.* **2007**, *28*,

2033−2038. (j) Runzi, T.; Guironnet, D.; Gottker-Schnetmann, I.; Mecking, S. Reactivity of Methacrylates in Insertion Polymerization. *J. Am. Chem. Soc.* **2010**, *132*, 16623−16630. (k) Schuster, N.; Rünzi, T.; Mecking, S. Reactivity of Functionalized Vinyl Monomers in Insertion Copolymerization. *Macromolecules* **2016**, *49*, 1172−1179. (l) Goodall, B. L. Late Transition Metal Catalysts for the Copolymerization of Olefins and Polar Monomers. *Top. Organomet. Chem.* **2009**, *26*, 159−178. (m) Xu, Y.-H.; Lu, J.; Loh, T.-P. Direct Cross-Coupling Reaction of Simple Alkenes with Acrylates Catalyzedby Palladium Catalyst. *J. Am. Chem. Soc.* **2009**, *131*, 1372−1373. (n) Chen, E. Y.-X. Coordination Polymerization of Polar Vinyl Monomers by Single-Site Metal Catalysts. *Chem. Rev.* **2009**, *109*, 5157−5214. (o) Cai, Z.; Do, L. H. Thermally Robust Heterobimetallic Palladium-Alkali Catalysts for Ethylene and Alkyl Acrylate Copolymerization. *Organometallics* **2018**, *37*, 3874−3882. (p) Wen, Z.-K.; Xu, Y.-H.; Loh, T.-P. Palladium-Catalyzed Cross-Coupling of Unactivated Alkenes with Acrylates: Application to the Synthesis of the C13-C21 Fragment of Palmerolide A. *Chem. - Eur. J.* **2012**, *18*, 13284−13287. (q) Zhang, Y.; Cui, Z.; Li, Z.; Liu, Z.-Q. Pd(II)-Catalyzed Dehydrogenative Olefination of Vinylic C-H Bonds with Allylic Esters: General and Selective Access to Linear 1,3-Butadienes. *Org. Lett.* **2012**, *14*, 1838−1841. (r) Wen, Z.-K.; Xu, Y.-H.; Loh, T.-P. Palladium(II)-catalyzed cross-coupling of simple alkenes with acrylates: a direct approach to 1,3-dienes through C-H activation. *Chem. Sci.* **2013**, *4*, 4520−4524. (s) Liu, M.; Yang, P.; Karunananda, M. K.; Wang, Y.; Liu, P.; Engle, K. M. C(alkenyl)-H Activation via Six-Membered Palladacycles: Catalytic 1,3-Diene Synthesis. *J. Am. Chem. Soc.* **2018**, *140*, 5805−5813. (t) Xin, B. S.; Sato, N.; Tanna, A.; Oishi, Y.; Konishi, Y.; Shimizu, F. Nickel Catalyzed Copolymerization of Ethylene and Alkyl Acrylates. *J. Am. Chem. Soc.* **2017**, *139*, 3611−3614. (u) Gao, J.; Yang, B.; Chen, C. Sterics versus electronics: Imine/phosphine-oxide-based nickel catalystsfor ethylene polymerization and copolymerization. *J. Catal.* **2019**, *369*, 233−238. (v) Ito, S.; Nozaki, K. Coordination-Insertion Copolymerization of Polar Vinyl Monomers by Palladium Catalysts. *Chem. Rec* **2010**, *10*, 315−325. (w) Li, M.; Wang, X.; Luo, Y.; Chen, C. A Second-Coordination-Sphere Strategy to Modulate Nickel- and Palladium-Catalyzed Olefin Polymerization and Copolymerization. *Angew. Chem., Int. Ed.* **2017**, *56*, 11604−11609. (x) Zhang, Y.; Mu, H.; Pan, L.; Wang, X.; Li, Y. Robust Bulky [P,O] Neutral Nickel Catalysts for Copolymerization of Ethylene with Polar Vinyl Monomers. *ACS Catal.* **2018**, *8*, 5963−5976. (y) Kanai, Y.; Foro, S.; Plenio, H. Bispentiptycenyl-Diimine-Nickel Complexes for Ethene Polymerization and Copolymerization with Polar Monomers. *Organometallics* **2019**, *38*, 544−551. (z) Liang, T.; Chen, C. Position Makes the Difference: Electronic Effects in Nickel-Catalyzed Ethylene Polymerizations and Copolymerizations. *Inorg. Chem.* **2018**, *57*, 14913−14919.

(4) (a) Keyes, A.; BasbugAlhan, H. E.; Ordonez, E.; Ha, U.; Beezer, D. B.; Dau, H.; Liu, Y.-S., Tsogtgerel, E.; Jones, G. R.; Harth, E. Olefins and Vinyl Polar Monomers: Bridging the Gap for Next Generation Materials. *Angew. Chem. Int. Ed.* **2019**, DOI: 10.1002/anie.201900650. (b) Boffa, L. S.; Novak, B. M. Copolymerization of Polar Monomerswith Olefins Using Transition-Metal Complexes. *Chem. Rev.* **2000**, *100*, 1479−1494. (c) Nakamura, A.; Ito, S.; Nozaki, K. Coordination-InsertionCopolymerization of Fundamental Polar Monomers. *Chem. Rev.* **2009**, *109*, 5215−5244. (d) Ito, S.; Munakata, K.; Nakamura, A.; Nozaki, K. Copolymerization of Vinyl Acetate with Ethylene by Palladium/Alkylphosphine-Sulfonate Catalysts. *J. Am. Chem. Soc.* **2009**, *131*, 14606−14607. (e) Chen, M.; Chen, C. A Versatile Ligand Platform for Palladium- and Nickel-Catalyzed Ethylene Copolymerization with Polar Monomers. *Angew. Chem., Int. Ed.* **2018**, *57*, 3094−3098. (f) Guironnet, D.; Caporaso, L.; Neuwald, B.; Göttker-Schnetmann, I.; Cavallo, L.; Mecking, S. Mechanistic Insights on Acrylate Insertion Polymerization. *J. Am. Chem. Soc.* **2010**, *132*, 4418−4426. (g) Guo, L. H.; Liu, W. J.; Chen, C. L. Late transition metal catalyzed G-olefin polymerization and copolymerization with polar monomers. *Mater. Chem. Front* **2017**, *1*, 2487−2494. (i) Sun, J.; Chen, M.; Luo, G.; Chen, C.; Luo, Y. Diphosphazane-monoxide and Phosphine-sulfonate Palladium Catalyzed Ethylene Copolymerization with Polar Monomers: A Computational Study. *Organometallics* **2019**, *38*, 638−646. (j) Johnson, L. K.; Wang, L.; McLain, S.; Bennett, A.; Dobbs, K.; Hauptman, E.; Ionkin, A.; Ittel, S.; Kunitsky, K.; Marshall, W.; McCord, E.; Radzewich, C.; Rinehart, A.; Sweetman, K. J.; Wang, Y.; Yin, Z. H.; Brookhart, M. Copolymerization of ethylene and acrylates by nickel catalysts. *ACS Symp. Ser.* **2003**, *857*, 131−142. (k) Liang, T.; Chen, C. Side-Arm Control in Phosphine-Sulfonate Palladium- and Nickel-Catalyzed Ethylene Polymerization and Copolymerization. *Organometallics* **2017**, *36*, 2338−2344. (l) Trost, B. M.; Imi, K.; Davies, I. W. Elaboration of Conjugated Alkenes Initiated by Insertion into a Vinylic C-H Bond. *J. Am. Chem. Soc.* **1995**, *117*, 5371−5372. (m) Tan, C.; Chen, C. Emerging Palladium and Nickel Catalysts for Copolymerization of Olefins with Polar Monomers. *Angew. Chem., Int. Ed.* **2019**, *58*, 7192−7200. (h) Tan, C. Emerging Palladium and Nickel Catalysts for Copolymerization of Olefins with Polar Monomers. *Angew. Chem., Int. Ed.* **2019**, *38* (37), 997−1010.

(5) Zarrouki, A.; Espinosa, E.; Boisson, C.; Monteil, V. Free Radical Copolymerization of Ethylene with Vinyl Acetate under Mild Conditions. *Macromolecules* **2017**, *50*, 3516−3523.

(6) Michalak, A.; Ziegler, T. DFT Studies on the Copolymerization of D-Olefins with Polar Monomers: Comonomer Binding by Nickel- and Palladium-Based Catalysts with Brookhart and Grubbs Ligands. *Organometallics* **2001**, *20*, 1521−1532.

(7) Williams, B. S.; Leatherman, M. D.; White, P. S.; Brookhart, M. Reactions of Vinyl Acetate and Vinyl Trifluoroacetate withCationic DiiminePd(II) and Ni(II) Alkyl Complexes:Identification of Problems Connected with Copolymerizationsof these Monomers with Ethylene. *J. Am. Chem. Soc.* **2005**, *127*, 5132−5146.

(8) Adams, R. D.; Tedder, J. D. Formation of N,N-Dimethylacrylamide by a Multicenter Hydrocarbamoylation of C_2H_2 with N,N-Dimethylformamide Activated by $Ru_5(\mu_5\text{-}C)(CO)_{15}$. *Inorg. Chem.* **2018**, *57*, 5707−5710.

(9) Adams, R. D.; Akter, H.; Tedder, J. D. CH Activations in Aldehydes in Reactions with $Ru_5(\mu_5\text{-}C)(CO)_{15}$. *J. Organomet. Chem.* **2018**, *871*, 159−166.

(10) (a) Lewis, J.; Johnson, B. F. G. Some Aspects of the Chemistry of the Cluster Carbonyls of Osmium. *Gazz. Chim. Ital.* **1979**, *109*, 271−289. (b) Keister, J.; Shapley, J. R. The Interaction of $H_2Os_3(CO)_{10}$ with Alkenes. Intermediates in Hydrogenation and Carbon-HydrogenBond Activation. *J. Am. Chem. Soc.* **1976**, *98*, 1056−1057. (c) Keister, J.; Shapley, J. R. Reaction of Ethylene with the Unsaturated Cluster Complex $H_2Os_3(CO)_{10}$. *J. Organomet. Chem.* **1975**, *85*, C29−C31. (d) Nubel, P. O.; Brown, T. L. Photolysis of $Re_2(CO)_{10}$ in the Presence of Simple Olefins. Thermal Reactivity of (-Hydride)(—alkenyl)dirheniumOctacarbonyl Compounds. *J. Am. Chem. Soc.* **1984**, *106*, 644−652. (e) McGhee, W. D.; Hollander, F. J.; Bergman, R. G. C-H Oxidative Addition and Reductive Elimination Reactions in a Dinuclear Iridium Complex. *J. Am. Chem. Soc.* **1988**, *110*, 8428−8443.

(11) (a) Davies, H. M. L.; Beckwith, R. E. J. Catalytic enantioselective C-H activation by means of metal-carbenoid-induced C-H insertion. *Chem. Rev.* **2003**, *103*, 2861−2903. (b) Davies, H. M. L.; Jin, Q. L. Highly diastereoselective and enantioselective C-H functionalization of 1,2-dihydronaphthalenes: A combined C-H activation/cope rearrangement followed by a retro-cope rearrangement. *J. Am. Chem. Soc.* **2004**, *126*, 10862−10863. (c) Davies, H. M. L.; Manning, J. R. C-H Activation as a Strategic Reaction: Enantioselective Synthesis of 4-Substituted Indoles. *J. Am. Chem. Soc.* **2006**, *128*, 1060−1061. (d) Adams, C. S.; Boralsky, L. A.; Guzei, I. A.; Schomaker, J. M. Modular Functionalization of Allenes to AminatedStereotriads. *J. Am. Chem. Soc.* **2012**, *134*, 10807−10810. (e) Zalatan, D. N.; Du Bois, J. A Chiral Rhodium Carboxamidate Catalyst for Enantioselective C-H Amination. *J. Am. Chem. Soc.* **2008**, *130*, 9220−9221. (f) Zalatan, D. N.; Du Bois, J. Understanding the Differential Performance of $Rh_2(esp)_2$ as a Catalyst for C-H Amination. *J. Am. Chem. Soc.* **2009**, *131*, 7558−7559.

(12) Adams, R. D.; Smith, M. D.; Tedder, J. D. Substituent-Directed Activation of CH bonds in Activated Olefins by $Ru_5(\mu_5\text{-}C)(CO)_{15}$. *Eur. J. Inorg. Chem.* **2018**, *2018*, 2984−2986.

(13) Komiya, S.; Ito, T.; Cowie, M.; Yamamoto, A.; Ibers, J. A. Carbon-Hydrogen Bond Activation by Transition MetalComplexes. Oxidative Addition of Alkyl Methacrylateto Ruthenium. The Structure of Hydrido(2-n-butoxycarbonylpropenyl-C1,0)tris-(triphenylphosphine)ruthenium(II). *J. Am. Chem. Soc.* **1976**, *98*, 3874−38841.

(14) Mingos, D. M. P.; May, A. S. In *The Chemistry of Metal Cluster Complexes*. Shriver, D. F., Kaesz, H. D., Adams, R. D., Eds.; VCH Publishers: New York, 1990; Ch. 2.

(15) Boyar, E.; Deeming, A. J.; Rothwell, I. P.; Henrick, K.; McPartlin, M. Chelation of Vinyl Acetate and Related Unsaturated Ketones: Molecular Structure of $[Os\{_3(CO)_{10}(CH_2{=}CHOCOMe)]$. *J. Chem. Soc., Dalton Trans.* **1986**, 1437−1441.

(16) Vrieze, K. In *Dynamic Nuclear Magnetic Resonance Spectroscopy*; Jackman, L. M.; Cotton, F. A.; Academic Press: New York, 1975; Ch. *11*, Sec. II.D.2.

(17) Binch, G. In *Dynamic Nuclear Magnetic Resonance Spectroscopy*; Jackman, L. M.; Cotton, F. A.; Academic Press: New York, 1975; Ch. *3*, Sec. II.B.

(18) (a) Szajek, L. P.; Lawson, R. J.; Shapley, J. R. The “Indenyl Effect” on Ethylene Rotation in Iridium(I) Complexes. *Organometallics* **1991**, *10*, 357−361. (b) Albietz, P. J., Jr.; Cleary, B. P.; Paw, W.; Eisenberg, R. Cationic Complexes of Iridium: Diiodobenzene Chelation, Electrophilic Behavior with Olefins, and Fluxionality of an Ir(I) Ethylene Complex. *Inorg. Chem.* **2002**, *41*, 2095−2108. (c) Yan, X.; Einstein, F. W. B.; Sutton, D. *Can. J. Chem.* **1995**, *73*, 939−955. (d) Batchelor, R. J.; Einstein, F. W. B.; Lowe, N. D.; Palm, B. A.; Yan, X.; Sutton, D. (Pentamethylcyclopentadienyl)nitrosyl(ethylene)-iridium Tetrafluoroborate, $[(\eta^5\text{-}C_5Me_5)Ir(NO)(C_2H_4)][BF_4]$: Synthesis, Characterization, and Some Reactions. X-ray Crystal Structures of the Title Compound and Its Derivatives $(\eta^5\text{-}C_5Me_5)Ir(NO)\text{-}(CH_2CH_2OEt)$ and $(\eta^5\text{-}C_5Me_5)_2$ $lr_2X_2(\mu\text{-}X)(\mu\text{-}NO)$ (X = Br, I). *Organometallics* **1994**, *13*, 2041−2052. (e) Mlekuz, M.; Bougeard, P.; Sayer, B. G.; McGlinchey, M. J.; Rodger, C. A.; Churchill, J. W.; Ziller, J.; Kang, S.-W.; Albright, T. A. X-ray Crystal Structure and Molecular Dynamics of (Indenyl)bis(ethylene)rhodium(I): 500-MHz NMR Spectra and EHMO Calculations. *Organometallics* **1986**, *5*, 1656−1663. (f) Kakkar, A. K.; Taylor, N. J.; Calabrese, J. C.; Nugent, W. A.; Roe, D. C.; Connaway, E. A.; Marder, T. B. An unusual rotational distortion in an $[(\eta\text{-indenyl})\ RhL_2]$ complex: molecular structures of $[(\eta\text{-}1,2,3\text{-}Me_3C_9H_4)Rh(\eta\text{-}C_2H_4)_2]$ and $[(\eta\text{-}C_9H_7)Rh(CO)_2]$. *J. Chem. Soc., Chem. Commun.* **1989**, 990−992.

(19) Rouquet, G.; Chatani, N. Catalytic Functionalization of $C(sp^2)$-H and $C(sp^3)$-H Bonds by Using Bidentate Directing Groups. *Angew. Chem., Int. Ed.* **2013**, *52*, 11726−11743.

(20) (a) De Sarkar, S.; Liu, W.; Kozhushkov, S. I.; Ackermann, L. Weakly Coordinating Directing Groups for Ruthenium(II)- Catalyzed C-H Activation. *Adv. Synth. Catal.* **2014**, *356*, 1461−1479. (b) Ackermann, L. Carboxylate-Assisted Ruthenium-Catalyzed Alkyne Annulations by C-H/Het-H Bond Functionalizations. *Acc. Chem. Res.* **2014**, *47*, 281−295.

(21) (a) Engle, K. M.; Mei, T.-S.; Wasa, M.; Yu, J.-Q. Weak Coordination as a Powerful Means for Developing Broadly Useful C-H Functionalization Reaction. *Acc. Chem. Res.* **2012**, *45*, 788−802. (b) Engle, K. M.; Yu, J.-Q. Developing Ligands for Palladium(II)-Catalyzed C-H Functionalization: Intimate Dialogue between Ligand and Substrate. *J. Org. Chem.* **2013**, *78*, 8927−8955.

(22) Johnson, B. F. G.; Lewis, J.; Nicholls, J. N.; Puga, J.; Raithby, P. R.; Rosales, M. J.; McPartlin, M.; Clegg, W. The Synthesis of $[Ru_5C(CO)_{15}]$ by the Carbonylation of $[Ru_6C(CO)_{17}]$ and the Reactions of the Pentanuclear Cluster with a Variety of Small-Molecules: the X-Ray Structure Analyses of $[Ru_5C(CO)_{15})]$,$Ru_5C\text{-}(CO_{15})(MeCN)]$, $[Ru_5C(CO)_{14}(PPh_3)]$, $[Ru_5C(CO_{13})(PPh_3)_2]$ and $[Ru_5(\mu\text{-}H)_2C(CO_{12})(Ph_2P(CH_2)_2PPh_2)]$. *J. Chem. Soc., Dalton Trans.* **1983**, 277−290.

(23) Bailey, P. J.; Braga, D.; Dyson, P. J.; Grepioni, F.; Johnson, B. F. G.; Lewis, J.; Sabatino, P. The Synthesis, Molecular Structure and lnterconversion of Two Novel Benzene-coordinated Pentaruthenium-Carbido Cluster Isomers $[Ru_5C(CO)_{12}(\mu_3{:}\eta^2{:}\eta^2{:}\eta^2\text{-}C_6H_6)]$ and $[Ru_5C(CO)_{12}(\eta^6\text{-}C_6H_6)]$. *J. Chem. Soc., Chem. Commun.* **1992**, 177−178.

(24) *APEX3 Version 2016.5-0 and SAINT Version 8.34A*; Bruker AXS, Inc.: Madison, WI, USA.

DOI: 10.1021/acs.inorgchem.9b00399
Inorg. Chem. 2019, 58, 8357−8368